

MOL # 100222

**Bitopic S1P<sub>3</sub> Antagonist Rescue from Complete Heart Block: Pharmacological and Genetic  
Evidence for Direct S1P<sub>3</sub> Regulation of Mouse Cardiac Conduction**

M. Germana Sanna, Kevin P. Vincent, Emanuela Repetto, Nhan Nguyen, Steven J. Brown,  
Lusine Abgaryan, Sean W. Riley, Nora B. Leaf, Stuart M. Cahalan, William B. Kiosses, Yasushi  
Kohno, Joan Heller Brown, Andrew D. McCulloch, Hugh Rosen, and Pedro J. Gonzalez-Cabrera

Departments of Chemical Physiology (M.G.S., E.R., N.N., H.R., P.J.G-C); Immunology (N.B.L.),  
and Molecular and Cellular Neuroscience (S.M.C.); The Scripps Research Institute Molecular  
Screening Center (S.B., L.A., S.W.R.); The Microscopy Core (W.B.K.), The Scripps Research  
Institute, 10550 N. Torrey Pines Rd., La Jolla, CA 92037; Kyorin Pharmaceutical Company,  
LTD (Y.K.), Tokyo, Japan; Departments of Bioengineering (A.D.M., K.P.V.) and Pharmacology  
(J.H.B.), University of California, San Diego, 9500 Gilman Dr., □La Jolla, CA 92093

MOL # 100222

**Running Title:** S1P<sub>3</sub> regulation of murine complete heart block.

**Corresponding Authors:** Hugh Rosen and Pedro J. Gonzalez-Cabrera, Department of Chemical

Physiology, The Scripps Research Institute, 10550 N. Torrey Pines Rd., La Jolla, CA 92037,

[hrosen@scripps.edu](mailto:hrosen@scripps.edu)

[gonzalp@scripps.edu](mailto:gonzalp@scripps.edu)

The number of text pages – 28

Number of Figures – 5

Number of Supplemental Figures - 11

Number of References - 40

Number of words in the Abstract - 241

Introduction – 635

Discussion – 1092

**Abbreviations:** S1P, Sphingosine 1-Phosphate; CCS, cardiac conduction system; CHB, complete heart block; AVN, Atrioventricular node; SAN, Sinoatrial node; KI, knockin; ECG, electrocardiogram

MOL # 100222

## ABSTRACT

The molecular pharmacology of the G-protein coupled receptors for Sphingosine 1-Phosphate (S1P) provides important insight into established and new therapeutic targets. A new, potent bitopic S1P<sub>3</sub> antagonist, SPM-354, with *in vivo* activity has been used, together with S1P<sub>3</sub>-knockin and -knockout mice to define spatial and functional properties of S1P<sub>3</sub> in regulating cardiac conduction. We show that S1P<sub>3</sub> is a key direct regulator of cardiac rhythm both *in vivo* and in isolated perfused hearts. FTY720 (2-amino-2-[2-(4-octylphenyl)ethyl]propane-1,3-diol) *in vivo*, and S1P in isolated hearts, induced a spectrum of cardiac effects ranging from sinus bradycardia to complete heart block, as measured by surface ECG in anesthetized mice, and in volume-conducted Langendorff preparations. Agonist effects on complete heart block are absent in S1P<sub>3</sub>-knockout mice, and are reversed, in wild type mice, with SPM-354, characterized and described here. Homologous knockin of S1P<sub>3</sub>-mCherry is fully functional pharmacologically, and is strongly expressed, by IHC confocal microscopy, in HCN4-positive atrioventricular node and His-Purkinje fibers, with relative less expression in HCN4-positive sinoatrial node. In Langendorff studies, at constant pressure, SPM-354 restored sinus rhythm in S1P-induced complete heart block, and fully reversed S1P mediated bradycardia. S1P<sub>3</sub> distribution and function in the mouse ventricular cardiac conduction system suggest a direct mechanism for heart block risk that should be further studied in humans. A richer understanding of receptor and ligand usage in the pacemaker cells of the cardiac system is likely to be useful in understanding ventricular conduction in health, disease and pharmacology.

MOL # 100222

## INTRODUCTION

Five high affinity G-protein coupled receptors for S1P have been identified (Rosen et al., 2013) and the crystal structure of S1P<sub>1</sub> has been solved (Hanson et al., 2012). This receptor cluster is medically important because the non-selective S1P-R (S1P<sub>1,3,4,5</sub>) modulator prodrug fingolimod (FTY720) is an effective oral therapy for the treatment of relapsing, remitting multiple sclerosis, by altering lymphocytic and central functions (Cohen et al., 2010; Kappos et al., 2010). Five (S1P<sub>1-5</sub>) subtypes that differ in spatial distribution, coupling and function can, singly or in combination, play complex roles in embryonic formation of the arterial media, blood pressure regulation and cardiac function (reviewed in Mendelson et al., 2014). For example, FTY720 in man is associated with significant sinus bradycardia and prolongation of the QTc interval (Schmouder et al., 2006; Kappos et al., 2010; Espinosa and Berger, 2011; Yagi et al., 2014). FTY720 treatment has additionally revealed increased incidence of atrioventricular (AV) disturbances during the first dose, including AV block and asystole, particularly in subgroups of patients with pre-existing cardiac conditions that require other therapeutics, i.e., beta blockers, calcium channel blockers, to maintain adequate cardiovascular dynamics (Vanoli et al., 2014). Atropine reversal of the sinus bradycardia (Kovarik et al., 2008) and the demonstration of sinus bradycardia with S1P<sub>1/5</sub>-selective agonists in man (Legangneux et al., 2013), as well as rodents (Fryer et al., 2012), suggest that SAN effects and those events resulting from alterations in AV-nodal conduction might be distinctly regulated.

There is little evidence to date concerning actual protein expression for the distinct S1P-R subtypes in the mammalian cardiac conduction system (CCS), a highly differentiated, neural-crest derived system responsible for initiating (SAN) and propagating (AVN and His-Purkinje system) synchronous cardiac contractions. Pharmacologically, S1P-R activation by S1P, FTY720

MOL # 100222

and selective S1P<sub>1/5</sub> agonists all induce cardiac depression, both at the level of the SAN (Guo et al., 1999), as well as by activating cardiomyocyte S1P<sub>1</sub> GIRK channel currents (Bunemann et al., 1995; Fryer et al., 2012; Legangneux et al., 2013). At the AVN level, in rats, FTY720 was recently shown to elevate the PR-interval duration, or total AV conduction time, which defines 1<sup>st</sup> degree AV block (Egom et al., 2015). In the same study, the authors also demonstrated the presence of S1P<sub>1-3</sub> transcripts in AVN, suggesting for a direct link between FTY720's PR-interval augmentation and S1P<sub>1-3</sub> engagement in situ.

The analysis of *in vivo* S1P<sub>3</sub> cardiac function can be confounded by its high expression on vascular smooth muscle (Forrest et al., 2004), where functionally, can result in vasoconstriction to S1P (Salomone 2003, 2008), or in the case with FTY720, an acute overall increase in total peripheral resistance (Fryer et al., 2012). Consistent with a role of S1P<sub>3</sub> in vasoconstriction, Murakami et al., (2010) demonstrated that the coronary flow (CF) rate reduction observed following S1P perfusion, in rat Langendorff heart preparations, was fully sensitive to S1P<sub>3</sub> antagonist reversal.

The detailed understanding of S1P<sub>3</sub> signaling in the CCS remains incomplete. We have approached the problem of defining receptor usage in distinct and highly differentiated cell populations that are difficult to study *ex vivo*, by building a tool set of both genetic and pharmacological tools that together define S1P<sub>3</sub> distribution and function. In this report we characterize a novel bitopic S1P<sub>3</sub> antagonist, SPM-354, that competes for binding in both the orthosteric and allosteric sites as defined by the natural ligand, and the selective allosteric S1P<sub>3</sub> agonist, CYM-5541, respectively (Parrill et al., 2000; Schuerer et al., 2008; Jo et al., 2012). Using SPM-354, the S1P<sub>1</sub> selective antagonist W146 (Sanna et al., 2006) and fluorescence-tagged S1P<sub>3</sub>-mCherry knockin (KI) mice, in concert with the previously described S1P<sub>3</sub> knockout (KO)

MOL # 100222

mouse (Ishii et al, 2001; Yang et al., 2002), we combined these systems to allow the roles of SIP<sub>3</sub> causal expression, and its functional consequences in the CCS, to be more clearly defined.

MOL # 100222

## MATERIALS AND METHODS

**Synthesis of SPM-354.** SPM-354 was synthesized as follows: 1) (122 mg, 0.164 mmol, Supplemental Figure 1) was dissolved in MeCN (2 mL) and Iodotrimethylsilane (117  $\mu$ L, 0.822 mmol) was slowly added at 0°C under argon atmosphere. After stirring for 30 min at 0°C, the reaction mixture was poured into water (10 mL), and then the resultant mixture was stirred for 1 h at 0°C. The precipitate was filtered, washed with water, and dried in vacuo at 50 °C. The crude residue was dissolved in MeOH and stirred for 30 min at RT, then the mixture was filtered and insoluble materials were washed with MeOH (5 mL). The filtrate was concentrated in vacuo. The residue was suspended in MeCN, stirred for 30 min at RT, then the resultant precipitate was filtered, washed with MeCN, and dried in vacuo at 50°C to give SPM-354 (50 mg, 0.0973 mmol) as a colorless powder. mp: 156-159 °C.  $[\alpha]_{D25} -7.67$  (c 0.50, MeOH).  $^1\text{H NMR}$  (DMSO- $d_6$ - $d_4$ TFA, 400 MHz):  $\delta$  0.90 (3H, t, J = 7.3 Hz), 1.26-1.40 (2H, m), 1.54- 1.66 (2H, m), 1.70-1.82 (2H, m), 2.61-2.75 (2H, m), 3.86-3.97 (2H, m), 7.10 (1H, d, J = 7.9 Hz), 7.19 (1H, dd, J = 7.9, 1.8 Hz), 7.27 (1H, d, J = 1.8 Hz), 7.34 (1H, d, J = 7.9 Hz), 7.40 (1H, d, J = 1.8 Hz), 7.56 (1H, d, J = 8.6 Hz). HRESIMS (+): 514.08255 (Calcd. for C<sub>20</sub>H<sub>25</sub>ClF<sub>3</sub>NO<sub>5</sub>PS, 514.08317). Ana. Calcd for C<sub>20</sub>H<sub>24</sub>ClF<sub>3</sub>NO<sub>5</sub> PS. 0.1H<sub>2</sub>O: C, 46.74%; H, 4.71%; N, 2.73%. Found: C, 46.58%; H, 4.73%; N, 2.72%. SPM-354 is reference example 47 in WO2011004604.

**SPM-354 selectivity.** Receptor activation through Beta-arrestin recruitment (TANGO<sup>TM</sup>, Life Technologies) was used to determine SPM-354 selectivity. U2OS cells stably expressing individual S1P receptors (S1P<sub>1-5</sub>) were seeded on 384-well plates at 10,000 cells per well, and incubated for 48 h according to the manufactures' protocol. SPM-354 in 1% fatty acid free BSA was added at the indicated concentrations to incubate for 1 h. The S1P or selective S1P<sub>3</sub> agonist

MOL # 100222

CYM-5541 concentrations were added to the wells, and incubated for 4 h at 37°C followed by addition of LiveBLAzer™ reagent. Following 2 h, the plates were read on an EnVision™ (Perkin Elmer) plate reader to measure S1P or CYM-5541 activity - Blue (410 nm excitation, 460 emission) to Green (410 excitation, 535 emission) - ratios. For Schild analyses in S1P<sub>1</sub> and S1P<sub>3</sub> cells, the S1P or CYM-5541 concentration response curves were fit using sigmoidal nonlinear regression in GrahPad Prism software, and the resulting EC50 values compared to no-ligand controls to generate the dose ratios (DR). These were graphed in the Schild's plot vs. the log [M] of SPM-354, yielding the pA2 values.

**Animals.** Experiments were conducted in accordance with the National Institutes of Health Guide for the Care and Use of Laboratory Animals, following approved protocols by the Institutional Animal Care and Use Committee at The Scripps Research Institute, La Jolla, CA, and the University of California San Diego. Wild type (WT) C57BL/6J male mice were obtained from TSRI in-house breeding colony. Experiments with KO and KI mice included 8-12-week old male, C57BL/6J background animals bred for at least 20 generations. Isolated heart experiments were conducted with 8-12 week old male C57BL/6J mice and obtained from The Jackson Laboratory and age-matched male KO mice.

***In vivo* ECG recordings.** ECGs were recorded in Avertin (240 mpk i.p) anesthetized mice using subcutaneous inserted electrodes. Recordings were performed on a PowerLab 8/35 (AD Instruments) data acquisition unit at 4-KHz sampling rate, and under a heat lamp. Reversal of single-dose FTY720-induced bradycardia by SPM-354 was assessed in mice pre-administered i.p. with 20 mpk FTY720 for 5h, following anesthesia and a baseline ECG period of 4-6 min. After



MOL # 100222

baseline determination, mice were challenged i.p. with either 40 mpk SPM-354 or vehicle (20 %  $\beta$ -cyclodextrin, Sigma Aldrich) with continuous recording until 12 min. For determination of RR- and PR-interval duration, we included those values at the end of baseline equilibration with those at the end of FTY720 treatment, taken from LabChart Pro® software (AD Instruments).

For FTY720 complete heart block (CHB) reversal experiments, WT mice, pre-treated with 20 mpk FTY720 for 5h were anesthetized as above, implemented for ECG recording, and challenged, at onset of appearance of consecutive P-waves without a sequential QRS complex, with either 80 mpk SPM-354 i.p. or 1 mpk atropine, and recorded further until 12-min.

For FTY720-propranolol CHB experiments, WT, KI or KO mice, were pretreated with 20 mpk FTY720 for 5h and challenged with 1 mpk S(-)(-)-propranolol (Sigma Aldrich) during the last hour of FTY720 incubation. Two-min prior anesthesia, mice were then treated i.p. with single 120 mpk dose of SPM-354 or equal volume of vehicle, and ECG recordings were further collected for 12 min.

Data are shown as means  $\pm$  S.E.M. Statistical analyses between conditions were done using unpaired, two-tailed t tests (95% confidence interval) or two-way repeated-measure analyses of variance followed by a Bonferroni test (GraphPad Prism, GraphPad Inc, CA).

**Isolated heart studies.** For volume conducted ECG studies, WT or S1P<sub>3</sub>-KO mouse hearts were excised from mice anesthetized with 2.5% isoflurane in 100% oxygen. After aortic cannulation, the hearts were perfused retrograde with a constant pressure (70 mmHg) Langendorff setup using 37°C heated, oxygenated Krebs-Henseleit solution as reported (Liao et al., 2012). The hearts were placed in a custom chamber containing 37°C-warmed perfusate with two electrodes and a ground lead for the recording of volume conducted ECG. The voltage signal was filtered,

MOL # 100222

amplified and 60 Hz noise removed (Hum Bug Noise Eliminator, Quest Scientific) before being digitized at 5000 Hz. Parallel measurements of CF rate were made using an in-line flow probe (Transonic Systems, Inc) and average flow rate (0.1 Hz low-pass filtered) was recorded. Volume conducted ECG and coronary flow rate data were analyzed with custom software in MATLAB. ECGs were further digitally filtered (250 Hz low-pass) for display.

Drug delivery from a 0.5 mg/ml stock of S1P (Avanti Polar Lipids, Inc) in 50mM Na<sub>2</sub>CO<sub>3</sub>-20% β-Cyclodextrin, 5 mg/ml SPM-354 stock in 20% β-cyclodextrin, 1mg/ml W146 (Avanti Polar Lipids, Inc) in in 50mM Na<sub>2</sub>CO<sub>3</sub>-20% β-Cyclodextrin or 1mM atropine (Sigma Aldrich), was done by dissolving stocks into 3-5 ml volumes of pre-warmed, gassed Krebs-Henseleit solution to be delivered to the perfusion line.

**Generation of *SIP<sub>3</sub><sup>mCherry/mCherry</sup>* mice.** Both 5' (4.5Kb) and 3' (3.5Kb) arms of Exon2 encoding for mouse *Slpr3* gene were cloned by PCR from BAC (RP24-69B23, C.H.O.R.I) into Psp72 backbone vector (Promega) and sequenced. mCherry (Clontec) and the loxP neomycin resistance cassette (CAN, a generous gift from Mario Capecchi) were subsequently added downstream from the coding sequence of *Slpr3*. The linearized construct was injected into clone Bruce4 (B4) embryonic stem cells (ES) derived from C57BL/6J mice. Homologous recombination was confirmed by Southern Blot using two different 5' probes. Correctly targeted C57BL/6J ES cells were injected into recipient C57BL/6J (B6 albino) blastocysts. The resulting chimeric animals were crossed to C57BL/6J mice. Heterozygotes were mated to generate homozygous mice. Genotyping was performed from genomic DNA extracted from tails by PCR using two reverse and a common forward primer. PCR was performed using Phire polymerase (NEB) with two reverse (BW) and a common forward primer (FW): P MCherry N1 686 BW: 5' TCA CCA TGG

MOL # 100222

TGG CGA CCG GTG GCT TGC A 3'; S1pr3 11322 BW: 5' AGG CTG AAA TGC GTT GGT GAC TCC TTG GGT 3'; S1pr3 11103 FW: 5' ATG CAG CCT GCC CTC GAC CCA AGC AGA AGT 3'. All mice used were between 8 and 12 weeks of age. *SIP<sub>3</sub><sup>mCherry/mCherry</sup>* mice were then crossed onto the *SIP<sub>1</sub><sup>eGFP/eGFP</sup>* mice strain (Cahalan et al., 2011) to generate the double homozygote (DH) mouse line *SIP<sub>3</sub><sup>mCherry/mCherry</sup> /SIP<sub>1</sub><sup>eGFP/eGFP</sup>*.

**Generation of anti mCherry monoclonal antibody for westerns and IHC.** Rat anti-mouse mcherry was generated at the TSRI Center for Antibody Development and Production, by i.p. immunization of Wistar rats with 50 ug of mCherry Fluorescent protein (Biovison) in 200ul of PBS/Sigma Adjuvant System (Sigma Aldrich), and two antigen boosts in PBS/ALUM 3 weeks apart. Antigen positive hybridomas were expanded, and a clone, 16D7, isolated after 3 rounds of limited dilution subcloning. Antibodies were further purified by Protein G chromatography. Clone 16D7 Rat anti-mCherry antibody is commercially available at Life Sciences (#M11217) and Kerafast (EST202).

**SIP<sub>3</sub>-mCherry expression via Western blotting.** Excised whole hearts from homozygous SIP<sub>3</sub>-KI mice or SIP<sub>3</sub>-KO mice were rinsed in cold PBS, minced, and homogenized in RIPA buffer with HALT™ protease inhibitor cocktail (Pierce). Lysate processing, protein determination, SDS-PAGE and blotting were performed as reported in Cahalan et al., 2011. SIP<sub>3</sub>-mCherry expression was detected using 30 ug protein per lane with the anti-mCherry primary (1:1,000) described above, followed by rat HRP secondary (Jackson) with ECL Plus™ (GE Healthcare).

MOL # 100222

**Perfusion, tissue sectioning and immunohistochemistry of mouse heart.** Sample preparation for staining was performed as follows: mice were euthanized by CO<sub>2</sub> asphyxiation and perfused through the heart with Z-fix (Anatech). Hearts were harvested and fixed in Z-fix for 1 h and placed into 30% sucrose/PBS solution for 48 h at 4°C. Samples were frozen in blocks of OCT (Tissue Tek) with dry ice and ethanol. 40-100 µm sections were cut using a Microtome (Microm HM 550). Immunohistochemistry sections were permeabilized in PBS + 0.5% Triton X-100 (PBST) for 2 hours at RT; blocked in PBST for 2h at RT with 5% normal goat serum, washed 3 times in PBST and incubated for 12 h at 4° C with primary antibody (1:100) diluted in PBST + 1% normal goat serum. Primary incubation was followed by washing (3 times) in PBST, incubated with secondary antibody in PBST at 1:1,000 dilution for 2 h at RT, washed 3 times in PBS, stained for 1 h with DAPI (1:500), and mounted on Vectashield (Vector Laboratories) for confocal microscopy. The following primary antibodies were used for staining: anti-mCherry, anti-GFP (Abcam, ab6556), CD31 (Abcam, ab2836), Cyclic Nucleotide-Gated K<sup>+</sup> Channel 4, HCN4 (Santa Cruz, sc-28750) and Pan-Neuronal (Millipore, MAB2300). Secondaries: Alexa 555 (A21434), Alexa 633 (A21071), Phalloidin 488 (A12371) and DAPI-Nuclear stain (Life Technologies).

**Confocal Microscopy.** Confocal images were obtained with a Zeiss LSM 780 laser Scanning Confocal Microscope and processed with Zen 2012 Software (both Carl Zeiss Inc). Z stacks of images (obtained at 0.3 µm optical slice increments) were collected sequentially using a 63x objective, and then maximum projected into single flattened stacks for figure panels. In some cases, Z stacks were additionally imported into IMARIS software (Bitplane Inc) for 3D rendering.

MOL # 100222

## RESULTS

**SPM-354 ligand.** SPM-354 (Figure 1A), a 2-propyl substituent of previously described S1P<sub>3</sub> antagonist, SPM-242 (Jo et al., 2012), was found to be 6-10 fold more potent than SPM-242 for antagonizing S1P-S1P<sub>3</sub>  $\beta$ -arrestin recruitment (Supplemental Figure 2A), and to be 30-fold more potent on S1P<sub>3</sub> vs. S1P<sub>1</sub> (Supplemental Figure 2B). In S1P<sub>3</sub> cells, and similar to bitopic antagonist, SPM-242, SPM-354 was shown to be non-competitive against the selective allosteric S1P<sub>3</sub> agonist, CYM-5541 (PA<sub>2</sub> =  $-9.01 \pm 0.45$ , slope =  $1.34 \pm 0.32$ , n=3, Supplemental Figure 2C). SPM-354 had a margin of selectivity of 1,840-fold vs. S1P<sub>2</sub>, 8,000-fold vs. S1P<sub>4</sub> and 20,000-fold vs. S1P<sub>5</sub> for inhibiting S1P- $\beta$ -arrestin activation. SPM-354 was chosen for in vivo studies over SPM-242 due to its improved stability in vivo (the half-life in mouse is 6.7 h, Y. Kohno, personal communication), and allowed for a more effective in vivo probe of S1P<sub>3</sub> function.

**A role for S1P<sub>3</sub> in regulating cardiac rate and rhythm *in vivo*.** First-dose FTY720 administration in man is known to reduce heart rate, and in some cases, induce acute episodes of AV block (Vargas and Perumal, 2013). To further understand the contribution of S1P<sub>3</sub> in cardiac rhythm, we employed surface ECG analysis under Avertin anesthesia, in conjunction with FTY720 and SPM-354. Avertin was chosen because it is well tolerated in mice (Roth et al., 2002; Chu et al., 2006), and allowed for capture of high quality ECG waveforms. Heart rate plots show that administration of FTY720 to WT mice 5 h prior to anesthesia, produced significant bradycardia in all animals (n=7, p=0.0006, Figure 1B, top graph, red tracing) compared to water vehicle treatment (n=6, blue tracing). FTY720 induced bradycardia in WT mice was calculated from the RR interval on the ECG, showed significantly increased PR-interval duration from  $49 \pm 3$  msec at baseline to  $70 \pm 3$  msec after FTY720 treatment (p=0.0023, Figure 1C), indicative of

MOL # 100222

1<sup>st</sup> degree heart block. In contrast, and as expected (Sanna et al., 2004; Forrest, 2004), there were no measurable heart rate or ECG changes in KO mice treated with 20 mpk FTY720 (Figure 1B, bottom graph, red tracing and Figure 1D); despite KO mice having similar heart rate modulation maxima vs. WT following acute sympathetic and parasympathetic drug challenges (Supplemental Figure 3).

Additional experiments with the selective S1P<sub>1</sub> agonist CYM-5442, that has therapeutic efficacy in the experimental autoimmune encephalomyelitis models of multiple sclerosis (Gonzalez-Cabrera et al., 2008, 2012) produced no bradycardia when measured 5 h following 10 mpk i.p. administration (n=5, Fig. 1B, green tracing).

FTY720 induced bradycardia in WT mice was fully reversed, in a bimodal fashion, by the i.p. bolus injection of 40 mpk SPM-354 (p=0.001, Figure 1B, red tracing, light arrows), but not by 40 mpk i.p. injection of the S1P<sub>1</sub> antagonist W146 (n=5, Supplemental Figure 4). Furthermore, reversal of bradycardia by SPM-354 administration was associated with a partial, but not significant restoration of PR-interval elevation by FTY720 at protocol's end (p=0.17, Figure 1C). Parallel studies indicated that antagonist vehicle i.p. administration in FTY720 bradycardiac mice did not alter heart rate throughout the conditions ((p=0.148, n=6, Figure 1B, top graph, dark arrows), and importantly, 40 mpk SPM-354 treatment alone did not affect basal heart rate (p=0.090, n=4, Figure 1, blue line, light arrow), even when dosed up to 120 mpk (data not shown).

To our surprise, because mice are not known to be a highly arrhythmogenic species (Boukens et al., 2014) and because no descriptions of this FTY720 effect have been published, ~25 % of the mice receiving FTY720/Avertin developed signs of CHB, characterized by prolonged periods of at least 3 consecutive P-waves in the absence of a propagated QRS

MOL # 100222

ventricular conduction complex (ECG tracings, time point i, Figures 2B and 2C). This indicates that atrial depolarization remains intact but does not propagate through the AVN His-Purkinje fibers, to depolarize the ventricle. All the mice that underwent CHB (N=11) also displayed profound bradycardia ( $102 \pm 30$  bpm) prior to establishment of CHB. Importantly, in mice with established CHB, i.p. administration of 80 mpk SPM-354 (n=4, Figure 2C), but not 1 mpk of atropine (n=5, Figure 2B), after onset of CHB, led to acute rescue of QRS ventricular conduction within the first minute, and coupling to the atrial P-wave and restoration of sinus rhythm within 2-3 minutes (bottom ECG tracing). SPM-354 reversal of CHB was accompanied by a positive chronotropic response, which averaged  $370 \pm 28$  bpm at the end of the protocol. Mice administered with atropine, on the other hand, sustained deep bradycardia ( $85 \pm 55$  bpm at protocol's end) and CHB throughout the entire protocol. Moreover,  $\beta$ -cyclodextrin (vehicle) administration in two mice undergoing CHB, failed to revert the abnormal ECG to normal sinus rhythm (not shown).

**S1P<sub>3</sub> expression in the mouse cardiac conduction system.** We postulated that the appearance of CHB was a direct consequence of S1P-S1P<sub>3</sub>-mediated inhibition of ventricular conduction; therefore, we examined S1P<sub>3</sub> expression in cardiac tissues of KI mice by immunohistochemistry (IHC) confocal microscopy. Wild-type mouse S1P<sub>3</sub> was homologously replaced by KI of the coding sequence of mCherry to the immediate 3' end of *S1pr3* gene (Supplemental Figure 5). Homozygous KI mice were viable and fertile, were shown to express full length S1P<sub>3</sub>-mCherry in whole heart lysates by Western blot when probed with a monoclonal anti-mCherry antibody (Supplemental Figure 6A), and become lymphopenic to acute FTY720 treatment (Supplemental Figure 6C).

MOL # 100222

For IHC studies, we used HCN4 antibody to the cyclic nucleotide gated K channel, since it selectively labels all components of the CCS in adult mouse heart (Yamamoto et al., 2006; Harzheim et al., 2008; Kuratomi et al., 2009; Baruscotti et al., 2011). A confocal low power view of KI heart stained with anti-mCherry antibody for S1P<sub>3</sub> (red), HCN4, (green) and nuclei (blue) is shown in Figure 3A, with fields for subsequent high power imaging boxed (Supplemental Figure 7 includes high magnification panels of Figure 3A). Representative merged confocal images of SAN and AVN are shown (Figure 3B), together with associated differential interference (DIC) images (Supplemental Figure 8 includes high magnification panels of Figure 3B). The central artery of the SAN is readily seen (a, Figure 3B), with arterial smooth muscle expressing S1P<sub>3</sub>-mCherry. Obvious HCN4 staining of SAN is seen with a small number of interdigitating S1P<sub>3</sub>-mCherry positive processes. Atrioventricular node shows characteristic morphology on DIC and is strongly double positive for both S1P<sub>3</sub>-mCherry and HCN4 (see Supplemental Figure 8 for relative quantification of HCN4-and mCherry merged images in AVN and SAN). The Bundle of His, shown in cross section in Figure 3C, is also strongly double labeled for both HCN4 and S1P<sub>3</sub>-mCherry (a 3D isosurfacing IMARIS image is shown on the rightmost panel of Figure 3C). Additional IHC experiments using left ventricle heart sections from double-cross, S1P<sub>1</sub>-GFP x S1P<sub>3</sub>-mCherry, homozygous KI mice, showed S1P<sub>3</sub>-mCherry expression (red) in Purkinje fibers, as projections interdigitating between ventricular myocytes and coronary artery smooth muscle (Figure 3D, panel ii). A magnified image of a single Purkinje fiber further shows axonal -like projections wrapped around myocytes (Figure 3D, panel iii). In contrast, S1P<sub>1</sub>-GFP expression was, as expected (Cahalan et al., 2011), predominantly found on vascular endothelium (Figure 3D, panel i). mCherry positive projections could be double labeled with anti-mCherry mAb and Pan-neuronal markers (Supplemental Figure 9C), supporting the



MOL # 100222

neuronal origin of S1P<sub>3</sub> projections and their identification as Purkinje fibers. In addition, and as reported (Mazurais et al., 2002; Forrest et al., 2004), we found strong discrete S1P<sub>3</sub>-mCherry expression in vascular smooth muscle, differentiated from endothelial cells as shown in samples co-labeled with the endothelial marker CD31 (Supplemental Figure 9A and 9B).

**The incidence of FTY720 induced CHB can be increased to almost 100% by propranolol administration.** In order to assay the FTY720 induced CHB phenotype with a more robust protocol, we included the non-selective  $\beta$ -AR antagonist, propranolol, known to reduce heart rate and cardiac output in mice. FTY720-induced CHB was demonstrated by administering both FTY720 and propranolol as shown in Figure 4A. Under this protocol we studied the actions of vehicle or SPM-354 administration 2-min prior anesthesia. The establishment of CHB in FTY720/propranolol treated WT mice, with  $\beta$ -cyclodextrin vehicle pre-administration, prior anesthesia, increased to almost 100% (8 out of 9 mice displayed CHB throughout the protocol, Table 1), and, was associated with consistently low heart rates, usually below 100 bpm, as represented in the red tracing, Figure 4B. In parallel experiments, intraperitoneal injection of SPM-354 (120 mpk) 2-min prior anesthesia to WT mice with FTY720-propranolol, near completely prevented the establishment of CHB (7 out of 8 studied, Table 1) by maintaining sinus rhythm, and adequate heart rate as evidenced from the ECG pattern of SPM-354 pretreated mice, relative to vehicle (Figure 4C and 4D). Table 1 shows that when this protocol was applied to KO mice, there were no signs of CHB in the ECG (N=5), although KO mice were slightly bradycardic due to propranolol administration. No differences in heart rate were noted to administration of vehicles between WT and KO mice (WT baseline, 458 $\pm$ 12, WT end of recording, 443 $\pm$ 8; KO baseline 445 $\pm$ 17, KO end of recording, 423 $\pm$ 10). The FTY720 induction

MOL # 100222

of non-lethal bradycardia, and its reversal by SPM-354 (Sup. Fig 6B), as well as SPM-354 prevention of FTY720-propranolol induced CHB (Table 1), were also demonstrated in the S1P<sub>3</sub> KI mice, providing formal evidence for the normal pharmacological function of the tagged receptor KI.

**SPM-354 reverses S1P-induced normal ECG function and S1P-induced CHB in isolated, perfused hearts.** To differentiate between central or peripheral actions of SPM-354 CHB reversal *in vivo*, direct effects on cardiac rate and rhythm were studied in Langendorff preparations, with S1P as the ligand. For these studies, we tracked both the RR-interval duration along modulation of CF rate by the drugs, the latter, serving as internal control of S1P-S1P<sub>3</sub> function, and antagonist reversal (Murakami et al., 2010). We found that perfusion of increasing concentrations of S1P to isolated WT hearts reduced CF rate in a concentration dependent manner (Supplemental Figure 10A and 10B, N=4, EC<sub>50</sub> of  $0.80 \pm 0.14 \mu\text{M}$ ), which amounted to a 4.4-fold reduction, of 80% maximal response vs. baseline CF rate (Table 2, normal ECG values). According to previous reports of S1P-S1P<sub>3</sub> mediated coronary vasoconstriction, (Murakami et al, 2010), subsequent bolus of 3  $\mu\text{M}$  SPM-354 during maximal, 10  $\mu\text{M}$  S1P CF rate reduction, led to rapid reversal towards baseline CF rate, and in some cases, to above-baseline values (Supplemental Figure 10A). Complete tracking of the RR-interval duration in Supplemental Fig 10A shows that at 3  $\mu\text{M}$  S1P, there is a sharp increase in RR-interval duration, accompanied by segments of high inter beat variability, which appeared sustained at 10  $\mu\text{M}$  S1P, and like CF, were rapidly reversed to baseline values following 3  $\mu\text{M}$  SPM-354 perfusion (Table 2, normal ECG values).

MOL # 100222

Further analysis into S1P perfusion and cardiac rhythm variability was done using 3  $\mu$ M S1P, or an approximate EC80 of the S1P-mediated reduction in CF rate. In the Langendorff, S1P-induced arrhythmias are readily seen (Figure 5A), with the sequential transition from normal sinus rhythm at baseline, to gradual and steady bradycardia (not shown), then 2<sup>nd</sup> degree heart blocks with 2:1 and 3:1 atrioventricular conduction (S1P), and finally to CHB as shown by complete absence of QRS ventricular complexes. Figure 5A (Vehicle) demonstrates that vehicle perfusion to a heart with complete absence of QRS ventricular complexes does not induce reversal to normal rhythm, unlike subsequent perfusion with 3  $\mu$ M SPM-354 (end of tracing in Fig. 5A). Moreover, acute CHB (QRS complex suppression) following 3  $\mu$ M S1P perfusion was atropine resistant (Figure 5B), in contrast, in all 3 examples shown, perfusion with 3  $\mu$ M SPM-354 reverted the isolated CHB to sinus rhythm, accompanied by both compensatory tachycardia and restoration of CF rate to near baseline values (end of tracing in Figure 5B, Table 2, CHB values).

To formally exclude a role for S1P<sub>1</sub> in the CHB phenotype, additional experiments tested effects of S1P<sub>1</sub> antagonist W146 perfusion on S1P-induced CHB in WT hearts (Figure 5C). The data show that in established 3  $\mu$ M S1P-induced CHB, W146 perfusion at 10  $\mu$ M does not modify the abnormal cardiac rhythm whereas subsequent SPM-354 perfusion at 3  $\mu$ M, fully restored CHB to normal, steady waveform ECG in all 4 hearts studied.

To conclude that S1P-induced CHB was dependent on S1P<sub>3</sub>, we performed Langendorff experiments in hearts from S1P<sub>3</sub> KO mice (Supplemental Figure 11). Unlike WT (Supplemental Figure 11A), bolus perfusion of 3 $\mu$ M S1P to KO hearts (Supplemental Figure 11B) produced marginal elevations in RR-interval duration throughout the protocol, and, despite inducing

MOL # 100222

modest, albeit significant 30% acute inhibition in CF rate (Supplemental Figure 11C), S1P did not elicit measurable cardiac arrhythmias or CHB in KO hearts (n=7).

MOL # 100222

## DISCUSSION

This combination of genetic and pharmacological analyses in WT, receptor KO and KI mice provides multiple lines of evidence for S1P receptor subtype selective differential regulation of atrial and ventricular pacemaking and conduction events. S1P<sub>1</sub> has been shown to regulate sinus bradycardia, is coupled to GIRK (Guo et al., 2009), and is responsible for the atropine sensitive vagal sinus bradycardia (Kovarik et al., 2008; Fryer et al., 2012; Legangneux et al., 2013). S1P<sub>3</sub> in mice, has rich expression at mRNA level on cells of neural crest origin (Meng and Lee, 2009), and was recently shown to be transcriptionally present, along *Slpr1* and *Slpr2* transcripts, in the AVN of rats. We corroborate this finding in the KI mouse, and find expression of S1P<sub>3</sub>-mCherry on neural crest derived AVN, His bundles and cardiac Purkinje fibers, in addition to finding relatively high expression, as expected, on vascular smooth muscle in the coronary arteries (Forrest et al., 2004).

In mice, S1P<sub>3</sub> agonism by FTY720-P, as well as the chiral analog, AFD-R, produce bradycardia in WT but not in S1P<sub>3</sub>-deletant mice (Forrest et al., 2004; Sanna et al., 2004). Based on the KI IHC findings, and using proof-of-concept reversal of FTY720 bradycardia, we characterized a potent S1P<sub>3</sub> antagonist tool, SPM-354, to further query physiological functions of cardiac S1P<sub>3</sub> modulation.

We confirmed that FTY720 does not induce bradycardia in KO mice, whereas in bradycardic WT and/or KI mice pre-administered with FTY720, single-dose SPM-354 induced a significant positive, chronotropic response as shown previously by Murakami et al, 2011 with a separate S1P<sub>3</sub> antagonist.

Most important, we show first evidence of FTY720's arrhythmogenic potential in anesthetized WT mice, particularly in those mice experiencing severe bradycardia (<200 bpm)

MOL # 100222

due to FTY720 co-administration along beta-blocker, propranolol. Cardiac arrhythmias induced by FTY720-propranolol treatment in WT mice included episodes of CHB, where AV propagation of atrial depolarization is absent. Notably, 2-min prior-treatment with single-dose SPM-354 in FTY720-propranolol pre-treated WT and/or KI mice, largely prevented the establishment of CHB, while maintaining heart rate fairly constant, albeit low (approx. 200 bpm), and normal rhythm, throughout the protocol.

Lack of arrhythmias in S1P<sub>3</sub>-KO mice by FTY720-propranolol, coupled to the high S1P<sub>3</sub> IHC expression in mouse CCS, and prevention of CHB by the S1P<sub>3</sub> antagonist SPM-354 in WT and KI mice, provide support that arrhythmogenesis is strongly dependent on cardiac-intrinsic S1P<sub>3</sub> agonism. However in vivo limitations of the study precluding absolute interpretation of the 'origin' of the FTY720-induced conduction defects include: 1) possible modulation of other cardiac receptors (mouse heart expresses S1P<sub>1</sub>, S1P<sub>2</sub> and S1P<sub>5</sub>), 2) the known FTY720-mediated S1P<sub>3</sub> bronchoconstriction in mice, as shown by Trifilieff and Fozard, 2011, that would be relevant and potentially aggravated by coadministration of nonselective beta-blocker propranolol, and 3) use of an anesthetic.

The potential limitations are solved by measuring cardiac rate and rhythm directly in isolated hearts. We chose S1P for the Langendorff hung heart studies, rather than pro-drug FTY720, to avoid fingolimod's intrinsic requirement for kinase phosphorylation by Sphingosine-Kinase-2, to become an active agonist of S1P<sub>3</sub>, and to remove any potential for off-target effects of FTY720 such as SPLYase (Bandhuvula et al., 2005) and TRMP7 (Qin et al., 2013). These Langendorff studies provide the first evidence for direct S1P<sub>3</sub> cardiac intrinsic induction of lethal cardiac arrhythmias, including CHB, which are highly sensitive to reversal by S1P<sub>3</sub> antagonist SPM-354. To add validation to SPM-354 as an antagonist of S1P<sub>3</sub> with 30-fold higher potency

MOL # 100222

over S1P<sub>1</sub>, we measured CF rate reduction by S1P<sub>3</sub> agonism-and reversal thereof by SPM-354, since the S1P-S1P<sub>3</sub> axis reduces CF rate via coronary vasoconstriction. The data indicates that S1P induced arrhythmias presented sporadically, whereas CF rate reduction maxima and RR-interval elevation functions of S1P were universal. Moreover, SPM-354, and not the S1P<sub>1</sub> antagonist, W146, fully reversed all three functions of S1P perfusion, whereas CHB was atropine insensitive, and rapidly reversed by SPM-354, as similarly observed in the reversal of CHB with FTY720 *in vivo*.

Ischemia is not likely a significant factor in S1P-induced CHB. Specifically, we found that S1P infusion did not stop CF (E max = 0.80), allowing maintenance of residual constant pressure perfusion. In contrast, global ischemia models of arrhythmia require complete inhibition of CF for prolonged periods of 10 minutes or more. The onset of CHB in response to S1P or FTY720 and propranolol is very rapid (Fig. 4), and SPM-354-initiated recovery from acute CHB is equally rapid. Electrocardiographic evidence shows that SPM-354 first initiates an idioventricular rhythm in the first 60 seconds after infusion, followed by full coupling into sinus rhythm by minute 2. These ECG data support a direct effect on ventricular pacemaking cells and the rapidity of recovery reflects very effective and rapid perfusion of the ventricles in the face of CHB.

SPM-354 fits the definition of a bitopic ligand for S1P<sub>3</sub> based upon receptor kinetic studies. SPM-354 can compete for the published allosteric S1P<sub>3</sub> selective agonist CYM-5541 (Schuerer et al., 2008; Jo et al., 2012), as well as for the orthosteric agonist S1P, whereas CYM-5541 is unable to compete for the binding of the orthosteric S1P ligand (Jo et al., 2012). SPM-354 was chosen for *in vivo* studies over the previously described SPM-242 ligand, because it has improved *in vivo* efficacy. This stems from its 6-10 fold improvement in apparent K<sub>i</sub> as an S1P<sub>3</sub>

MOL # 100222

antagonist for which the (S)-enantiomer is essential to avoid agonism. In addition, SPM-242 with is 2-hydroxymethyl substituent, underwent very rapid phosphate ester hydrolysis in vivo, whereas the 2-propyl substituent in SPM-354 slows down the susceptibility to phosphohydrolases and enhances the half-life and persistence of SPM-354, allowing it to be a more effective in vivo probe of S1P<sub>3</sub> function.

In summary, modulation of S1P<sub>3</sub> activity is causally associated with AV nodal conduction block from three lines of evidence. First, S1P<sub>3</sub> must be present for induction of cardiac conduction changes by FTY720 and S1P, as deletion of *S1pr3* leads to mice being refractory to these agonist-induced changes. Second, the S1P<sub>3</sub> antagonist SPM-354 attenuates the failure of ventricular activation in nearly all mice with ECG signs of CHB by beta-blocker propranolol and FTY720 co-administration, and restores normal sinus rhythm. Third, S1P-induced CHB is replicated in Langendorff preparations and reversed by SPM-354 and not atropine or the S1P<sub>1</sub> antagonist W146.

S1P<sub>3</sub> distribution in mouse heart thus provides an insight into a potential mechanism-based cardiac risk that now prompts verification of S1P<sub>3</sub> expression in the human CCS. These new insights into S1P<sub>3</sub> usage in the pacemaker cells of the mouse heart, will enhance understanding of ventricular conduction physiology and pathology, particularly as pharmacological tools allow these data to be extended into larger animal species and man.



MOL # 100222

**AUTHORSHIP CONTRIBUTIONS:**

Participated in research design: H. Rosen, P.J. Gonzalez-Cabrera, M.G. Sanna, E. Repetto, S.M. Cahalan, J. Heller Brown, A. McCulloch, K.P. Vincent

Conducted experiments: P.J. Gonzalez-Cabrera, K.P. Vincent, M.G. Sanna, E. Repetto, W.B. Kiosses, S.J. Brown, L. Abgaryan, S.W. Riley, N.B. Leaf

Contributed new reagents or analytic tools: Y. Kohno; A. McCulloch

Performed data analysis: P.J. Gonzalez-Cabrera, K.P. Vincent, M.G. Sanna, W.B. Kiosses, S.J. Brown, L. Abgaryan, S.W. Riley

Wrote or contributed to the writing of the manuscript: H. Rosen, P.J. Gonzalez-Cabrera, M.G. Sanna, K.P. Vincent, S.J. Brown

MOL # 100222

## REFERENCES

Bandhuvula P., Tam, Y.Y., Oskouian B, Saba JD. (2005) The immune modulator FTY720 inhibits sphingosine-1-phosphate lyase activity, *J Biol Chem.* **280**, 33697-33700.

Baruscotti, M., Bucchi, A., Viscomi, C., Mandelli, G., Consalez, G., Gnecci-Rusconi, T., Montano, N., Casali, K. R., Micheloni, S., Barbuti, A., and DiFrancesco, D. (2011) Deep bradycardia and heart block caused by inducible cardiac-specific knockout of the pacemaker channel gene *Hcn4*, *Proc Natl Acad Sci U S A* **108**, 1705-1710.

Boukens BJ, Rivaud MR, Rentschler S, Coronel R (2014) Misinterpretation of the mouse ECG: 'musing the waves of *Mus musculus*'. *J Physiol.* **592**, 4613-4626.

Bunemann, M, Brandts, B, zu Heringdorf, D.M., van Koppen, C.J., Jakobs, K.H., Pott, L (1995) Activation of muscarinic K<sup>+</sup> current in guinea-pig atrial myocytes by sphingosine-1-phosphate *J Physiol*, **489**, 701–777.

Cahalan SM, Gonzalez-Cabrera PJ, Sarkisyan G, Nguyen N, Schaeffer MT, Huang L, Yeager A, Clemons B, Scott F, Rosen H (2011) Actions of a picomolar short-acting S1P<sub>1</sub> agonist in S1P<sub>1</sub>-eGFP knock-in mice. *Nat Chem Biol.* **7**:254-256.

Chu DK, Jordan MC, Kim JK, Couto MA, Roos KP (2006) Comparing isoflurane with tribromoethanol anesthesia for echocardiographic phenotyping of transgenic mice. *J Am Assoc Lab Anim Sci.* **45**:8-13.

MOL # 100222

Cohen JA, Barkhof F, Comi G, Hartung HP, Khatri BO, Montalban X, Pelletier J, Capra R, Gallo P, Izquierdo G, Tiel-Wilck K, de Vera A, Jin J, Stites T, Wu S, Aradhye S, Kappos L, (2010) TRANSFORMS Study Group Oral fingolimod or intramuscular interferon for relapsing multiple sclerosis. *N Engl J Med.* **362**:402-415.

Egom EE, Kruzliak P, Rotrekl V, Lei M (2015) The effect of the sphingosine-1-phosphate analogue FTY720 on atrioventricular nodal tissue. *J Cell Mol Med.* **19**:1729-1734.

Espinosa PS, Berger JR (2011) Delayed fingolimod-associated asystole. *Mult Scler;* **17**:1387-1389.

Forrest, M., Sun, S. Y., Hajdu, R., Bergstrom, J., Card, D., Doherty, G., Hale, J., Keohane, C., Meyers, C., Milligan, J., Mills, S., Nomura, N., Rosen, H., Rosenbach, M., Shei, G. J., Singer, II, Tian, M., West, S., White, V., Xie, J., Proia, R. L., and Mandala, S (2004) Immune cell regulation and cardiovascular effects of sphingosine 1-phosphate receptor agonists in rodents are mediated via distinct receptor subtypes, *The Journal of pharmacology and experimental therapeutics* **309**, 758-768.

Fryer, R. M., Muthukumarana, A., Harrison, P. C., Nodop Mazurek, S., Chen, R. R., Harrington, K. E., Dinallo, R. M., Horan, J. C., Patnaude, L., Modis, L. K., and Reinhart, G. A. (2012) The clinically-tested S1P receptor agonists, FTY720 and BAF312, demonstrate subtype-specific bradycardia (S1P(1)) and hypertension (S1P(3)) in rat, *PloS one* **7**, e52985.

MOL # 100222

Gonzalez-Cabrera, P. J., Jo, E., Sanna, M. G., Brown, S., Leaf, N., Marsolais, D., Schaeffer, M. T., Chapman, J., Cameron, M., Guerrero, M., Roberts, E., and Rosen, H. (2008) Full pharmacological efficacy of a novel S1P1 agonist that does not require S1P-like headgroup interactions. *Molecular pharmacology* **74**, 1308-1318.

Gonzalez-Cabrera, P. J., Cahalan, S. M., Nguyen, N., Sarkisyan, G., Leaf, N. B., Cameron, M. D., Kago, T., and Rosen, H. (2012) S1P(1) receptor modulation with cyclical recovery from lymphopenia ameliorates mouse model of multiple sclerosis. *Molecular pharmacology* **81**, 166-174.

Guo J, MacDonell KL, Giles WR (1999) Effects of sphingosine 1-phosphate on pacemaker activity in rabbit sinoatrial node cells. *Pflugers Arch.* 438:642-648.

Hanson, M. A., Roth, C. B., Jo, E., Griffith, M. T., Scott, F. L., Reinhart, G., Desale, H., Clemons, B., Cahalan, S. M., Schuerer, S. C., Sanna, M. G., Han, G. W., Kuhn, P., Rosen, H., and Stevens, R. C. (2012) Crystal structure of a lipid G protein-coupled receptor, *Science* **335**, 851-855.

Harzheim, D., Pfeiffer, K. H., Fabritz, L., Kremmer, E., Buch, T., Waisman, A., Kirchhof, P., Kaupp, U. B., and Seifert, R. (2008) Cardiac pacemaker function of HCN4 channels in mice is confined to embryonic development and requires cyclic AMP, *EMBO J* **27**, 692-703.

MOL # 100222

Ishii I, Friedman B, Ye X, Kawamura S, McGiffert C, Contos JJ, Kingsbury MA, Zhang G, Brown JH, Chun J (2001) Selective loss of sphingosine 1-phosphate signaling with no obvious phenotypic abnormality in mice lacking its G protein-coupled receptor, LP(B3)/EDG-3. *J Biol Chem*, **276**:33697-33704.

Jo, E., Bhatarai, B., Repetto, E., Guerrero, M., Riley, S., Brown, S. J., Kohno, Y., Roberts, E., Schurer, S. C., and Rosen, H. (2012) Novel selective allosteric and bitopic ligands for the S1P(3) receptor, *ACS chemical biology* **7**, 1975-1983.

Kappos, L., Radue, E. W., O'Connor, P., Polman, C., Hohlfeld, R., Calabresi, P., Selmaj, K., Agoropoulou, C., Leyk, M., Zhang-Auberson, L., Burtin, P., and Group, F. S. (2010) A placebo-controlled trial of oral fingolimod in relapsing multiple sclerosis, *The New England journal of medicine* **362**, 387-401.

Kovarik, J. M., Slade, A., Riviere, G. J., Neddermann, D., Maton, S., Hunt, T. L., and Schmouder, R. L. (2008) The ability of atropine to prevent and reverse the negative chronotropic effect of fingolimod in healthy subjects, *British journal of clinical pharmacology* **66**, 199-206.

Kuratomi, S., Ohmori, Y., Ito, M., Shimazaki, K., Muramatsu, S., Mizukami, H., Uosaki, H., Yamashita, J. K., Arai, Y., Kuwahara, K., and Takano, M. (2009) The cardiac pacemaker-specific channel Hcn4 is a direct transcriptional target of MEF2, *Cardiovasc Res* **83**, 682-687.

MOL # 100222

Legangneux, E., Gardin, A., and Johns, D. (2013) Dose titration of BAF312 attenuates the initial heart rate reducing effect in healthy subjects, *British journal of clinical pharmacology* **75**, 831-841.

Liao, R, Podesser, BK , Lim, CC (2012) The continuing evolution of the Langendorff and ejecting murine heart: new advances in cardiac phenotyping, *American Journal of Physiology - Heart and Circulatory Physiology* **303**:H156-H167.

Mazurais D, Robert P, Gout B, Berrebi-Bertrand I, Laville MP, Calmels T. (2002) Cell type-specific localization of human cardiac S1P receptors. *J Histochem Cytochem.* **50**:661-670.

Mendelson K, Evans T, Hla T (2014) Sphingosine 1-phosphate signalling. *Development.* **141**:5-9.

Meng, H., and Lee, V. M. (2009) Differential expression of sphingosine-1-phosphate receptors 1-5 in the developing nervous system, *Developmental dynamics : an official publication of the American Association of Anatomists* **238**:487-500.

Murakami A, Takasugi H, Ohnuma S, Koide Y, Sakurai A, Takeda S, Hasegawa T, Sasamori J, Konno T, Hayashi K, Watanabe Y, Mori K, Sato Y, Takahashi A, Mochizuki N, Takakura N (2010) Sphingosine 1-phosphate (S1P) regulates vascular contraction via S1P3 receptor: investigation based on a new S1P3 receptor antagonist. *Mol Pharmacol* **77**:704-713.

MOL # 100222

Parrill, A. L., Wang, D., Bautista, D. L., Van Brocklyn, J. R., Lorincz, Z., Fischer, D. J., Baker, D. L., Liliom, K., Spiegel, S., and Tigyi, G. (2000) Identification of Edg1 receptor residues that recognize sphingosine 1-phosphate, *The Journal of biological chemistry* **275**: 39379-39384.

Qin X, Yue Z, Sun B, Yang W, Xie J, Ni E, Feng Y, Mahmood R, Zhang Y, Yue L. Sphingosine and FTY720 are potent inhibitors of the transient receptor potential melastatin 7 (TRPM7) channels. (2013) *Br J Pharmacol*. 168:1294-1312.

Rosen, H., Stevens, R. C., Hanson, M., Roberts, E., and Oldstone, M. B. A. (2013) Sphingosine-1-Phosphate and Its Receptors: Structure, Signaling, and Influence, *Annual Review of Biochemistry* **82**:637-662.

Roth DM, Swaney JS, Dalton ND, Gilpin EA, Ross J Jr (2002) Impact of anesthesia on cardiac function during echocardiography in mice. *Am J Physiol Heart Circ Physiol*. **282**:H2134-H2140.

Salomone S, Potts EM, Tyndall S, Ip PC, Chun J, Brinkmann V, Waeber C (2008) Analysis of sphingosine 1-phosphate receptors involved in constriction of isolated cerebral arteries with receptor null mice and pharmacological tools, *Br J Pharmacol* **153**:140–147.

Salomone S, Yoshimura S, Reuter U, Foley M, Thomas SS, Moskowitz MA, Waeber C (2003) S1P3 receptors mediate the potent constriction of cerebral arteries by sphingosine-1-phosphate. *Eur J Pharmacol* **469**:125–134.

MOL # 100222

Sanna MG, Liao J, Jo E, Alfonso C, Ahn MY, Peterson MS, Webb B, Lefebvre S, Chun J, Gray N, Rosen H (2004) Sphingosine 1-phosphate (S1P) receptor subtypes S1P1 and S1P3, respectively, regulate lymphocyte recirculation and heart rate. *J Biol Chem* **279**:13839-13848.

Sanna MG, Wang SK, Gonzalez-Cabrera PJ, Don A, Marsolais D, Matheu MP, Wei SH, Parker I, Jo E, Cheng WC, Cahalan MD, Wong CH, Rosen H (2006) Enhancement of capillary leakage and restoration of lymphocyte egress by a chiral S1P1 antagonist *in vivo*. *Nat Chem Biol* **2**:434-441.

Schmouder, R., Serra, D., Wang, Y., Kovarik, J. M., DiMarco, J., Hunt, T. L., and Bastien, M. C. (2006) FTY720: placebo-controlled study of the effect on cardiac rate and rhythm in healthy subjects, *Journal of clinical pharmacology* **46**: 895-904.

Vargas WS, Perumal JS. (2013) Fingolimod and cardiac risk: latest findings and clinical implications. *Ther Adv Drug Saf.* **4**:119-124.

Yagi Y, Nakamura Y, Kitahara K, Harada T, Kato K, Ninomiya T, Cao X, Ohara H, Izumi-Nakaseko H, Suzuki K, Ando K, Sugiyama A (2014) Analysis of Onset Mechanisms of a Sphingosine 1-Phosphate Receptor Modulator Fingolimod-Induced Atrioventricular Conduction Block and QT-Interval Prolongation. *Toxicol Appl Pharmacol.* **281**:39-47.

Yang AH, Ishii I, Chun J (2002) In vivo roles of lysophospholipid receptors revealed by gene targeting studies in mice. *Biochim Biophys Acta.* **1582**:197-203.



MOL # 100222

Yamamoto, M., Dobrzynski, H., Tellez, J., Niwa, R., Billeter, R., Honjo, H., Kodama, I., and Boyett, M. R. (2006) Extended atrial conduction system characterised by the expression of the HCN4 channel and connexin45, *Cardiovasc Res* **72**:271-281.

MOL # 100222

## FOOTNOTES

This work was supported by the NIH grant [NIH 5U54 MH084512] to HR; Kyorin Pharmaceuticals grant [SFP-1499] to HR; and NIH grants [NIH 1RO1HL105242] and [1R03EB014593] to ADM.

M. Germana Sanna, Kevin P. Vincent, Emanuela Repetto equally contributed to this work.

MOL # 100222

## FIGURE LEGENDS

**Figure 1. S1P<sub>3</sub> dependent bradycardia by FTY720 treatment is associated with enhanced RR- and PR- interval duration that is reversed by SPM-354.** **A)** Chemical structure of SPM-354. **B)** Typical chronotropic responses in WT mice following 5 h treatment with vehicle, FTY720 or the S1P<sub>1</sub> agonist CYM-5442. The recordings show that a single i.p SPM-354 dose, but not antagonist vehicle, fully reverses FTY720 mediated bradycardia, without having a significant effect on heart rate when administered alone. The top graph shows that CYM-5442 does not significantly alter heart rate in WT mice at 5 h post administration. Absence of bradycardia by FTY720 in S1P<sub>3</sub> KO mice (**B**, lower graph). Bar graphs show mean  $\pm$  S.E.M. heart rates in WT and S1P<sub>3</sub> KO mice throughout baseline (BL), FTY720 (F), FTY720 + SPM-354 (F+S) or SPM-354 alone (S) conditions. Electrocardiographic waveforms in FTY720 treated mice display enhanced RR- and PR-interval duration in wild type (**C**) but not S1P<sub>3</sub> KO (**D**) mice, and partial restoration upon SPM-354 administration.

**Figure 2. FTY720 treatment increases the susceptibility for developing CHB.** Typical heart rate recordings and detailed ECGs of wild type mice undergoing CHB following 5 h 20 mpk FTY720 administration and anesthesia. (**A**) Protocol design. Single dose 120 mpk SPM-354 administration (**C**), but not atropine (**B**) at the onset of CHB, results in rapid reversal of FTY720 induced CHB within minutes. Detailed ECG analysis of mice undergoing FTY720 induced CHB have characteristic consecutive P-waves with absent QRS complexes. Representative ECG waveforms in FTY720 treated mice that while undergoing CHB, received either SPM-354 or

MOL # 100222

atropine. Same animal ECG recordings indicate the presence of CHB in both mice at time (i), and the outcome on cardiac rhythm post (ii) drug treatment.

**Figure 3. Immunohistology of S1P<sub>3</sub>-mcherry in the mouse cardiac conduction system.** Laser Scanning Confocal Fluorescence Images and DICs of whole heart, coronary artery, septum and Purkinje fibers of S1P<sub>3</sub>-mCherry KI mouse. **A)** Shows a mapped and multi-stitched composite of a typical whole heart section (10x objective, 40 panels) stained for S1P<sub>3</sub> (anti-mCherry/Alexa555, red), the cyclic nucleotide-gated K<sup>+</sup> channel 4, HCN4 (green), and nuclei (DAPI-Nuclear, blue). Signals strongly positive for S1P<sub>3</sub>-mCherry and HCN4 are clearly evident in the Purkinje-conduction system as indicated in the white rectangle box of the image. **B)** Examples of high-resolution multi-stack and maximum projected confocal images (63x), of the SA node and AV node are shown as both merged fluorescence and DIC image projections. S1P<sub>3</sub> (red) is significantly less expressed with HCN4 in the SA node and strongly expressed in the AV node. Nuclei are shown in blue and the sinoatrial nodal artery is indicated with an “a”. The IMARIS rendered images are also shown on the right panels. **C)** Cross section of the AV bundle labeled with same antibodies as in A and B. **D)** S1P<sub>3</sub> is localized in Purkinje fibers and in smooth muscle of S1P<sub>3</sub>-mCherry KI mouse heart. Panels show high resolution (63x) multi-stack and maximum projected Laser Scanning Confocal Fluorescence Images of cardiac smooth muscle cells (**i**), and Purkinje fibers (**ii** and **iii**), labeled with S1P<sub>3</sub> (anti-mCherry/Alexa555, red), S1P<sub>1</sub> (anti-GFP/Alexa633, green) and nuclei (DAPI, blue). S1P<sub>3</sub> is expressed in heart coronary artery smooth muscle and in Purkinje fibers, whereas S1P<sub>1</sub> is localized in the endothelium (**i**). The last panel series following the merged image shows a single snap shot image of a 3D surface rendered reconstruction of the fluorescent signals created with the IMARIS software.

MOL # 100222

Longitudinal sections of heart ventricular septum (**ii**) shows S1P<sub>3</sub> (red) staining of heart Purkinje fibers as projections interdigitating between ventricular myocytes. A magnified image (**iii**) of a single Purkinje fiber further shows axonal -like projections wrapped around myocytes. Nuclei are stained with DAPI (blue).

**Figure 4. The incidence of FTY720-induced CHB is increased by propranolol co-administration, requires S1P<sub>3</sub>, and is reversed by single-dose SPM-354 administration. A)**

Protocol schema. **B)** Representative heart rate recordings with magnified sections of the ECG at times (i) and (ii) of the recordings, in mice administered with FTY720/propranolol, and acutely pretreated with either vehicle (**B**, red tracing) or SPM-354 (**B**, blue tracing) 2-min prior to anesthesia. Vehicle pretreated, FTY720/propranolol mice, displayed deep bradycardia and irregular heart rate throughout having distinctive CHB episodes characteristic of consecutive P-waves with skipped QRS complexes(**C**). In comparison, SPM-354 pre-treated, FTY720/propranolol mice, displayed steady heart rate, with no signs of CHB as depicted in the magnified ECG taken at times (i) and (ii) of the recording (**D**). Table 1 includes the number of WT, S1P<sub>3</sub> KO and S1P<sub>3</sub> KI mice that underwent CHB under the protocol diagrammed on **A**, mean  $\pm$  S.E.M. heart rates at protocol's end, and the outcome of vehicle and/or SPM-354 administration on CHB establishment.

**Figure 5. SPM-354 reverses S1P induced CHB in ex-vivo mouse heart studies.**

Volume conducted ECGs were measured in isolated, unpaced, Langendorff perfused WT mouse hearts under constant pressure. The four rows for each panel contain representative 3-sec ECG tracings shown at baseline, 3-min following a bolus of 3  $\mu$  M S1P, 3-min following a bolus of

MOL # 100222

vehicle/W146 and 3-min following a bolus of SPM-354. After S1P introduction, baseline sinus rhythm (A-C; top row) degenerates into 2<sup>nd</sup>-degree AV-block with variable RR interval and eventually CHB (A-B; second row).  $\beta$ -cyclodextrin vehicle (**A**; third row), 1  $\mu$ M atropine (**B**; third row) and 10  $\mu$ M W146 (**C**; third row) fail to rescue S1P induced CHB, whereas SPM-354 (A-C; bottom row) restores AV conduction and returns the heart to normal sinus rhythm.

MOL # 100222

**Table 1.** Incidence of CHB and heart rates from in vivo FTY720 and propranolol administration in WT, KI and KO mice acutely pre-treated with either vehicle or SPM-354.

Treatment group	FTY720 + Propranolol (4h and 1h respectively)			
	<i>Acute 2-min Pretreatment</i>			
	Vehicle		SPM354	
	No. mice without CHB (Mice tested)	Heart Rate (BPM)	No. mice without CHB (Mice tested)	Heart Rate (BPM)
<b>Wild type</b>	1 (9)	N.D.	7 (8)	219 ± 12
<b>Knockin</b>	2 (7)	N.D.	4 (4)	148 ± 7.0
<b>Knockout</b>	5 (5)	350 ± 6.0	N.D.	N.D.

N.D. Not determined

MOL # 100222

**Table 2.** SPM-354 reverses S1P-induced RR interval augmentation and S1P-mediated CFR reduction in isolated perfused hearts of WT mice undergoing either normal ECG patterns, or those displaying CHB.

Treatment	Normal ECG		CHB	
	RR interval (msec)	CFR (ml/min)	RR interval (msec)	CFR (ml/min)
Baseline	177±35	1.31±0.31	168±7.6	1.33±0.40
+ S1P	351±164*	0.27±0.15*	620±177**	0.25±0.05*
+ SPM-354	156±42 <sup>n.s.</sup>	1.32±0.86 <sup>n.s.</sup>	205±31 <sup>a</sup>	1.65±0.54 <sup>n.s.</sup>

Baseline values were taken immediately following 5 min of heart equilibration from start of perfusion.

<sup>n.s.</sup>Not significant vs. Baseline

\*p<0.05 vs. Baseline

\*\*p<0.01 vs. Baseline

<sup>a</sup>p<0.05 vs. S1P



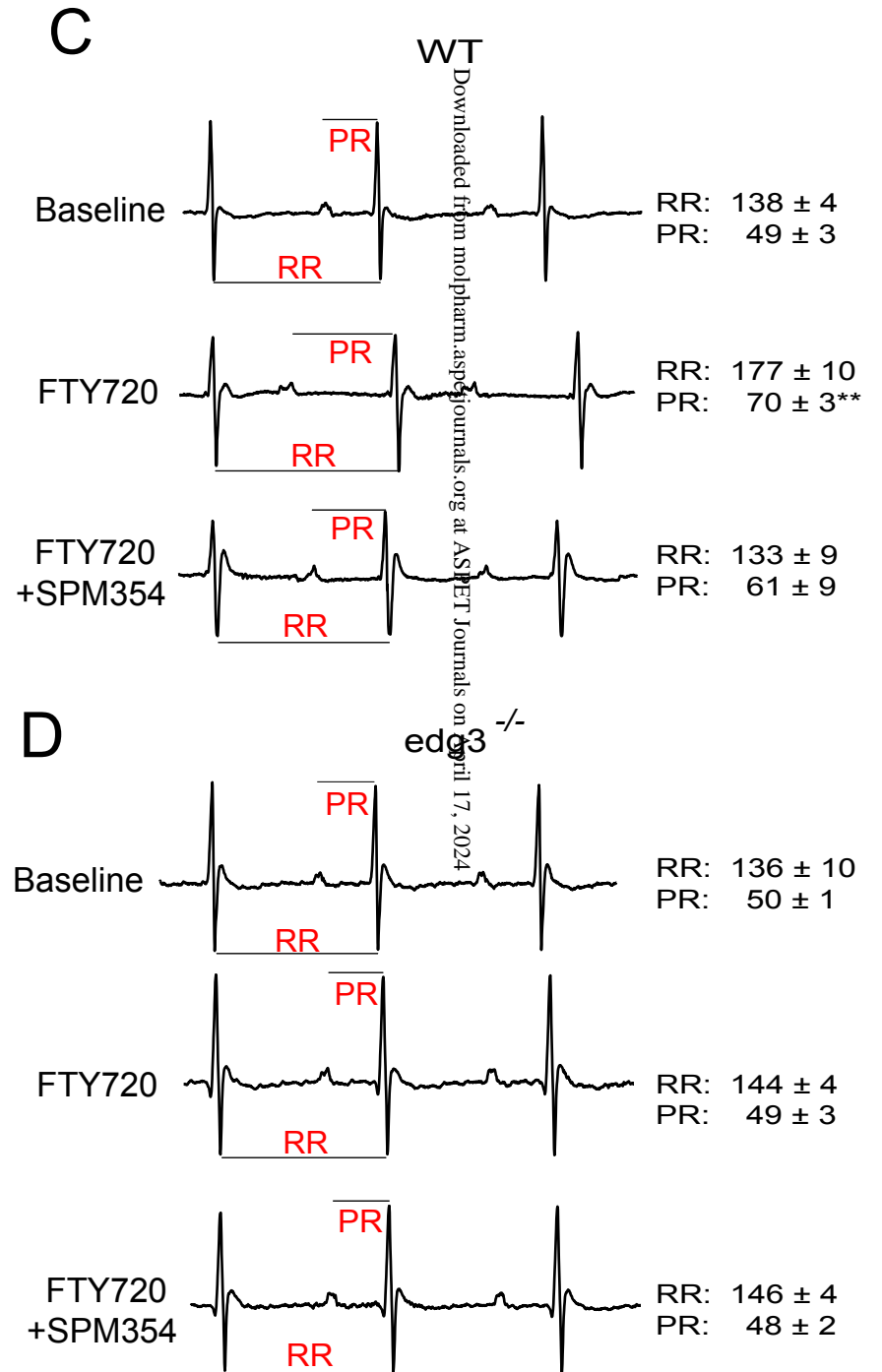
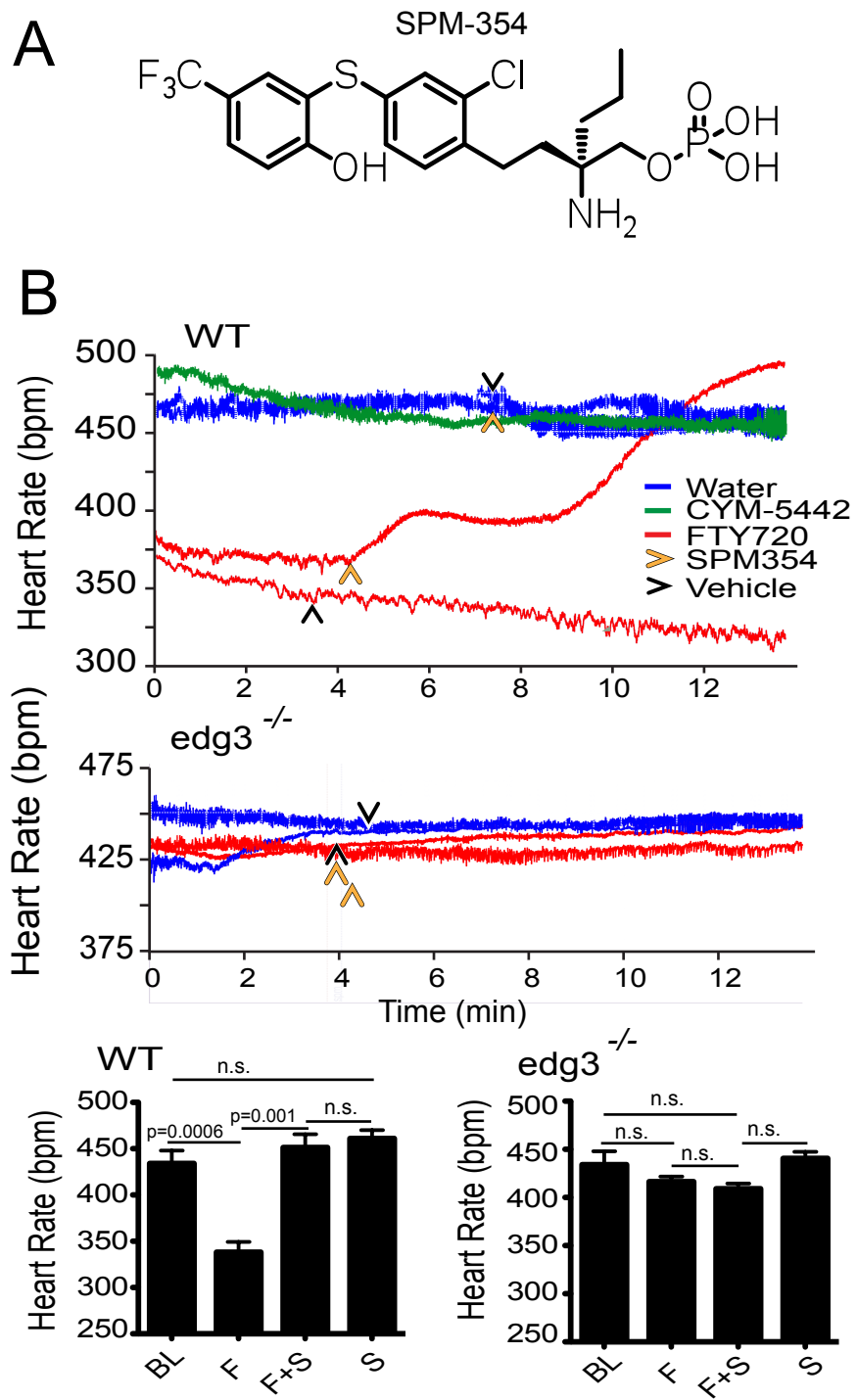


Figure 1

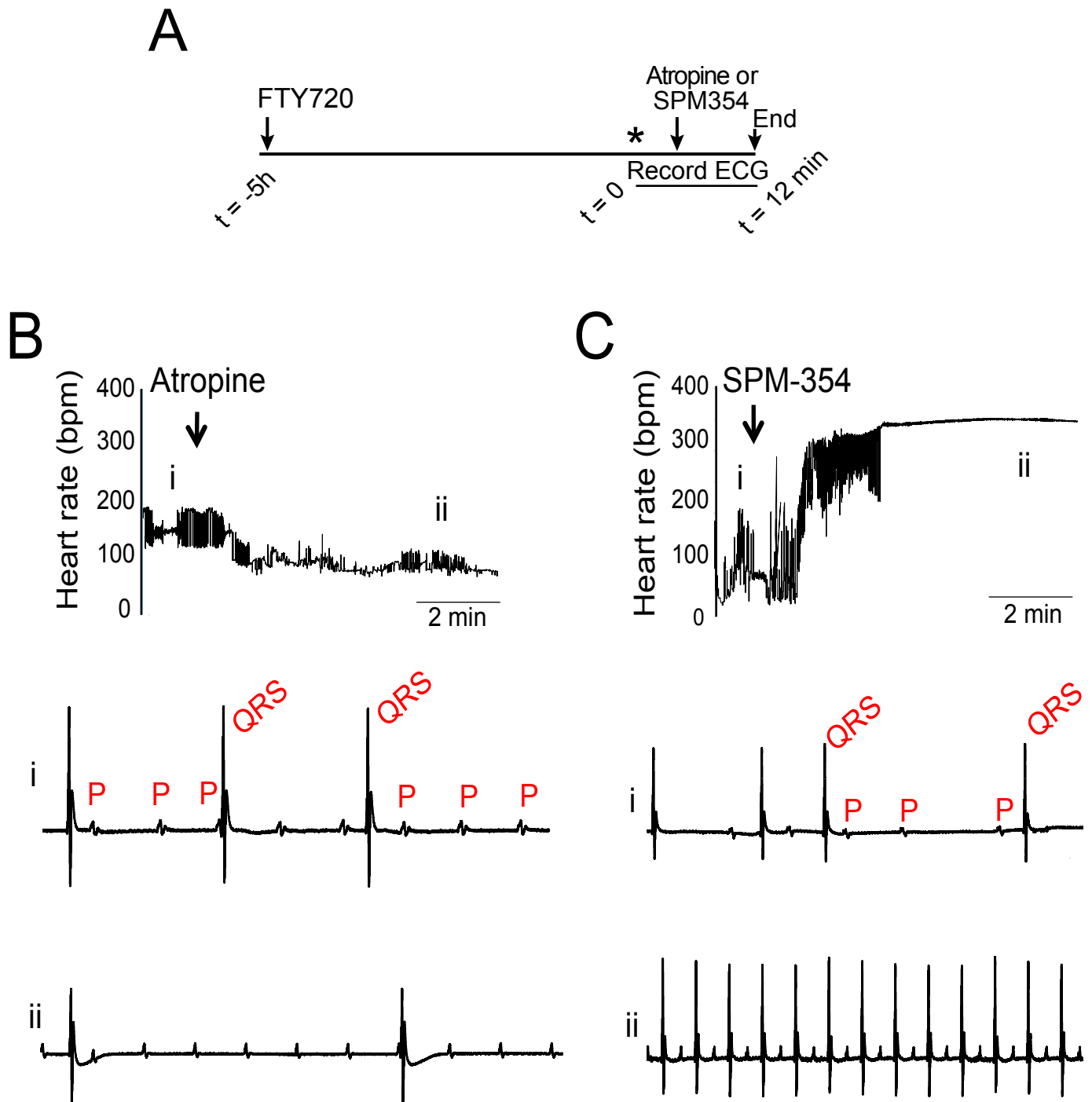


Figure 2

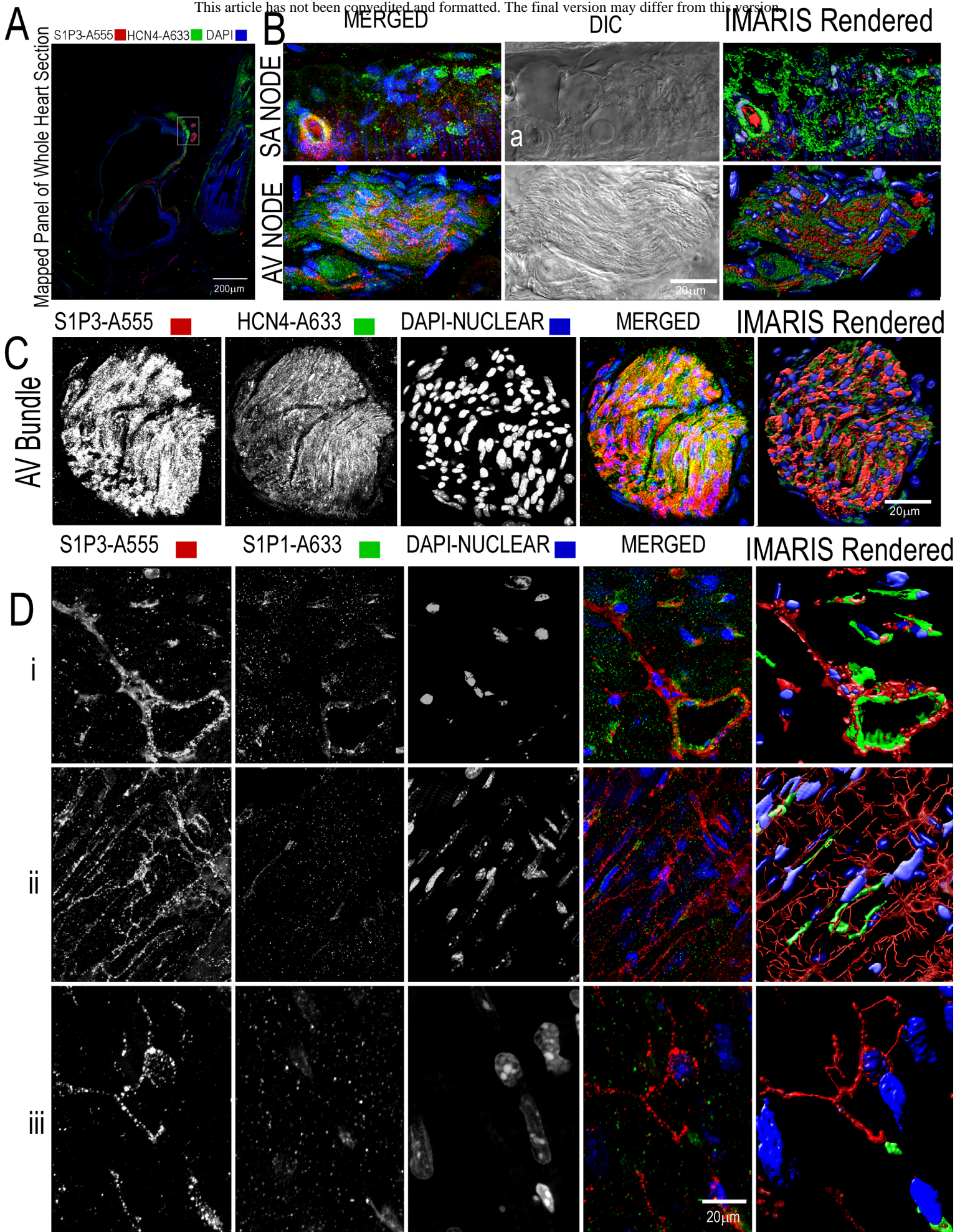


Figure 3

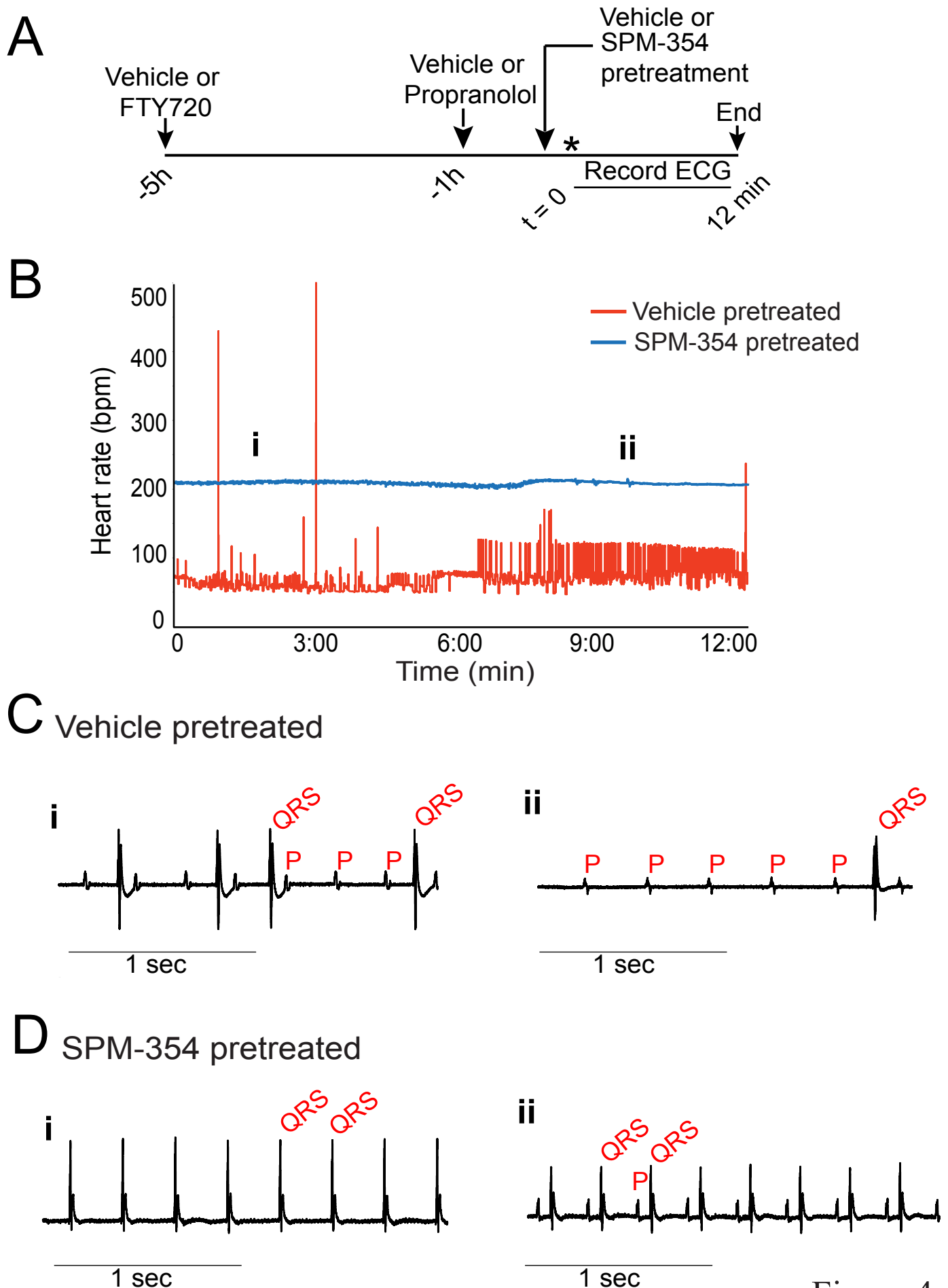


Figure 4

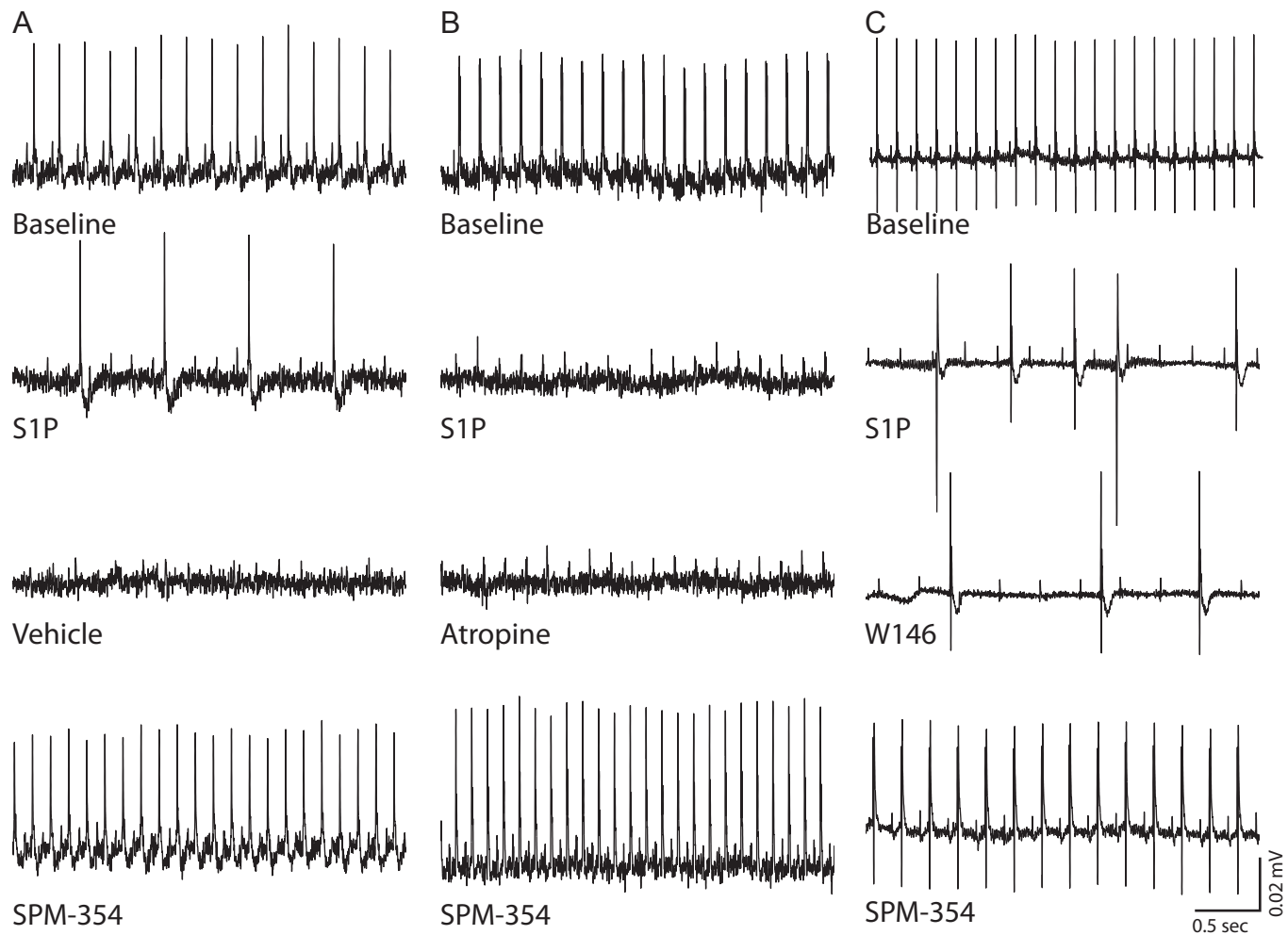


Figure 5

MOL Manuscript #100222

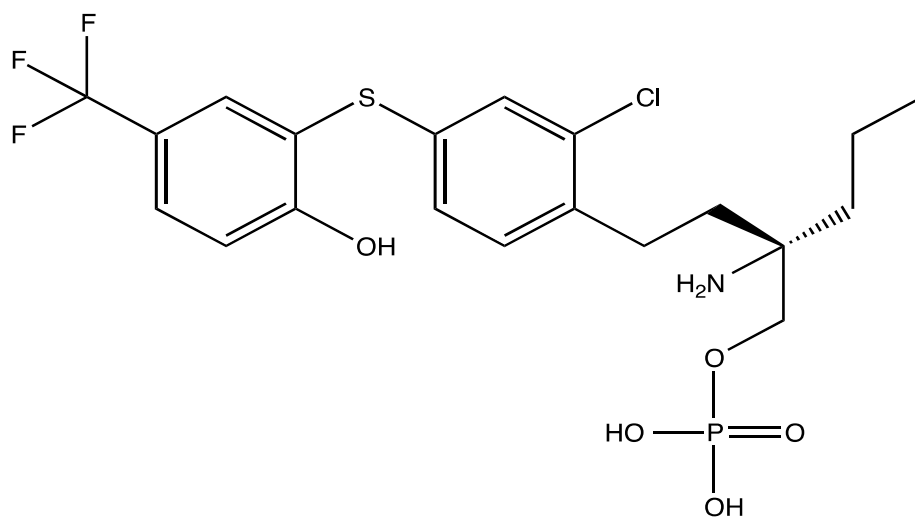
SUPPORTING INFORMATION

**Bitopic S1P<sub>3</sub> Antagonist Rescue from Complete Heart Block: Pharmacological and Genetic Evidence for Direct S1P<sub>3</sub> Regulation of Mouse Cardiac Conduction**

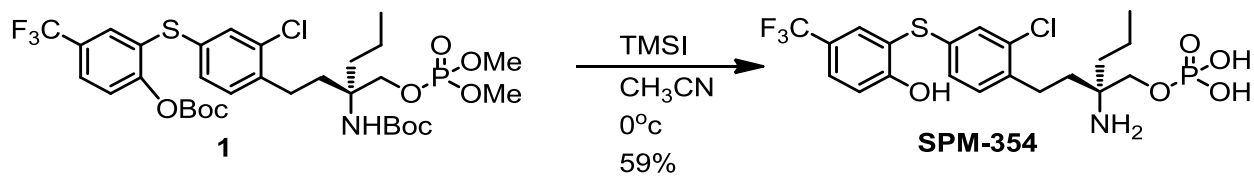
M. Germana Sanna, Kevin P. Vincent, Emanuela Repetto, Nhan Nguyen, Steven J. Brown, Lusine Abgaryan, Sean W. Riley, Nora B. Leaf, Stuart M. Cahalan, William B. Kiosses, Yasushi Kohno, Joan Heller Brown, Andrew D. McCulloch, Hugh Rosen, and Pedro J. Gonzalez-Cabrera

**MOLECULAR PHARMACOLOGY**

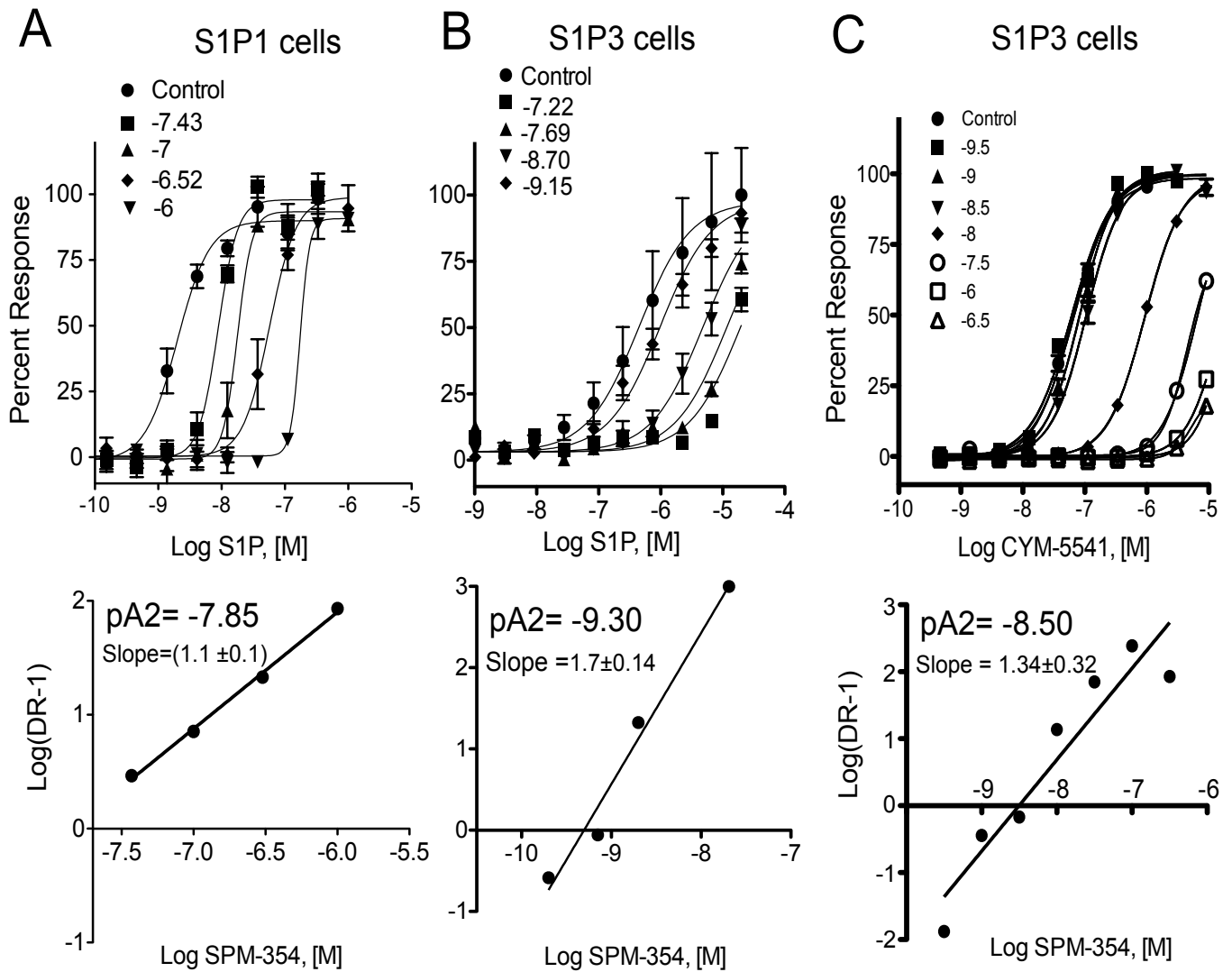
(S)-2-amino-4-[2-chloro-4-(2-hydroxy-5-trifluoromethylphenylthio)phenyl]-2-propylbutylphosphoric acid monoester



#### Experimental Section: Synthesis of **SPM-354**

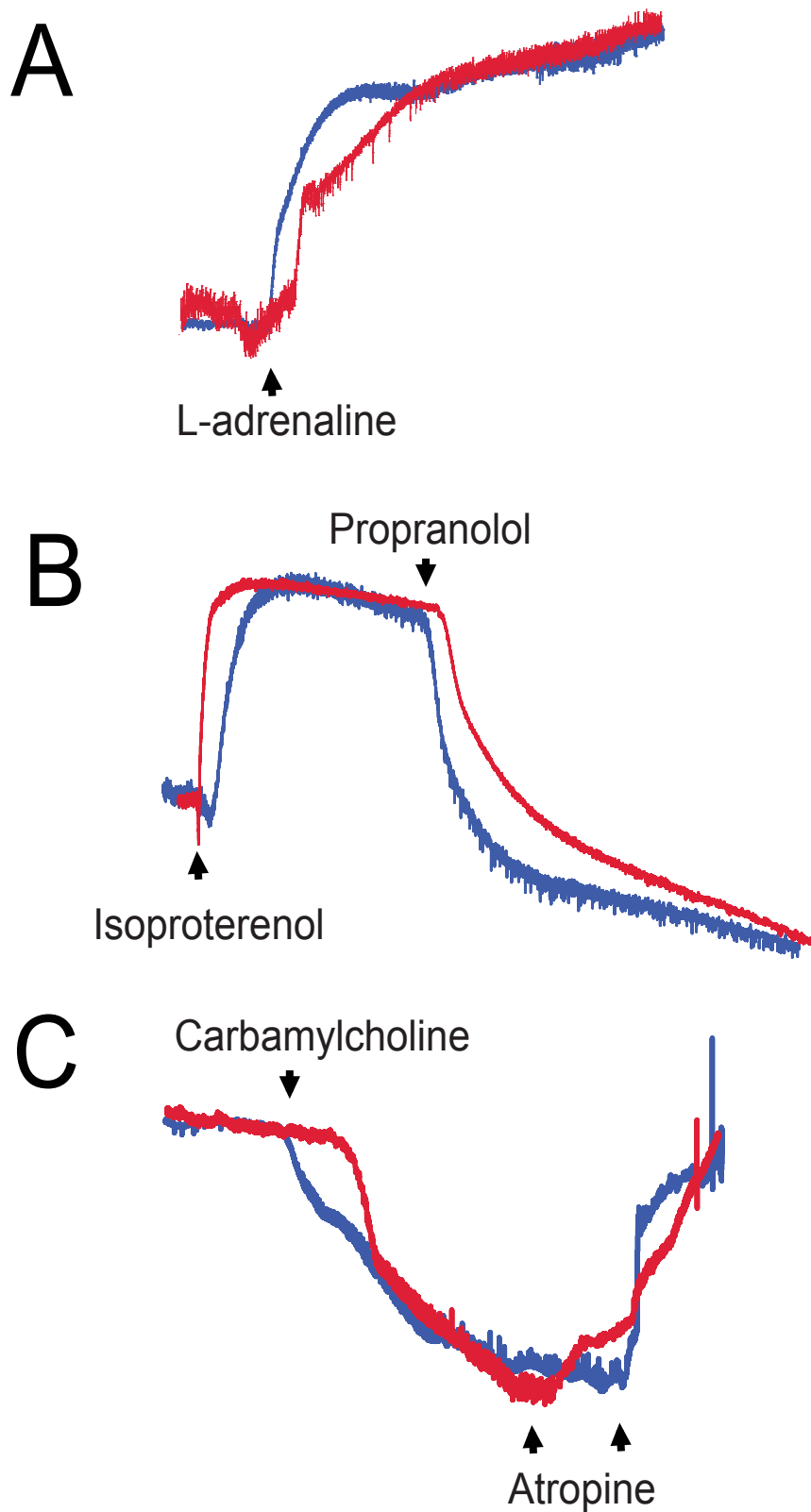


**Supplemental Figure 1.** Chemical structure and synthesis scheme for SPM-354.

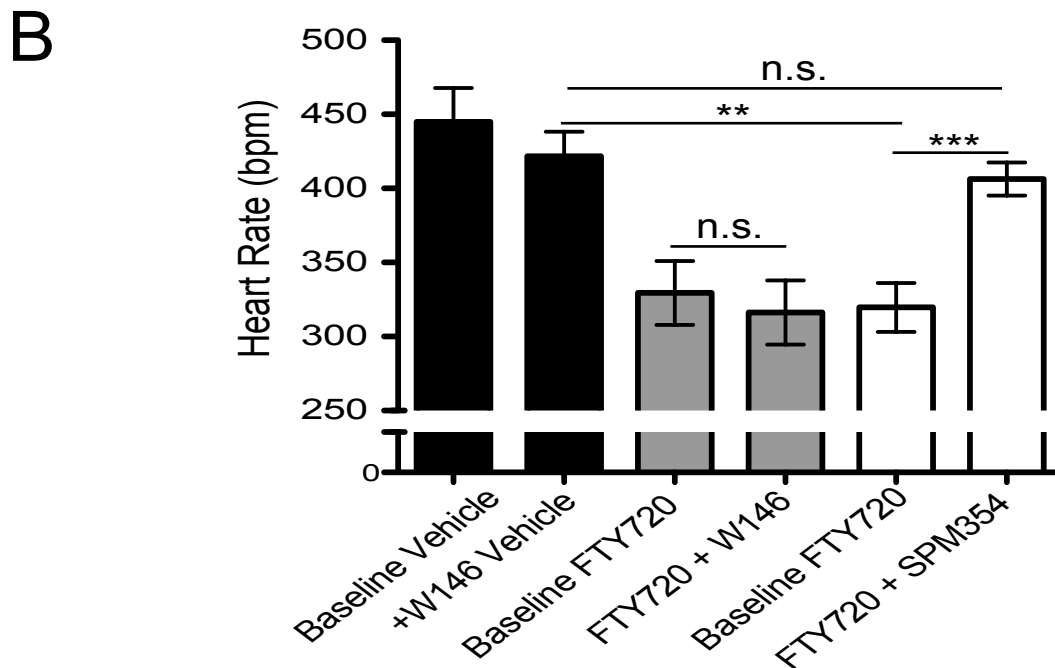
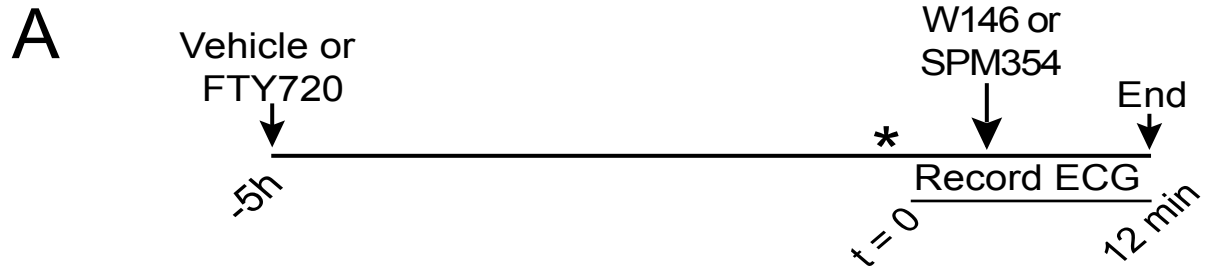


**Supplemental Figure 2.** Apparent affinities and slopes of SPM-354 for antagonizing Beta-arrestin recruitment by S1P in (A) S1P1 or (B) S1P3 cells, and CYM-5541-induced Beta-arrestin recruitment in S1P3 cells. For each of the curves, agonist concentrations were added in triplicate; n=2 for experiments in A; n=3 for experiments in B and C.

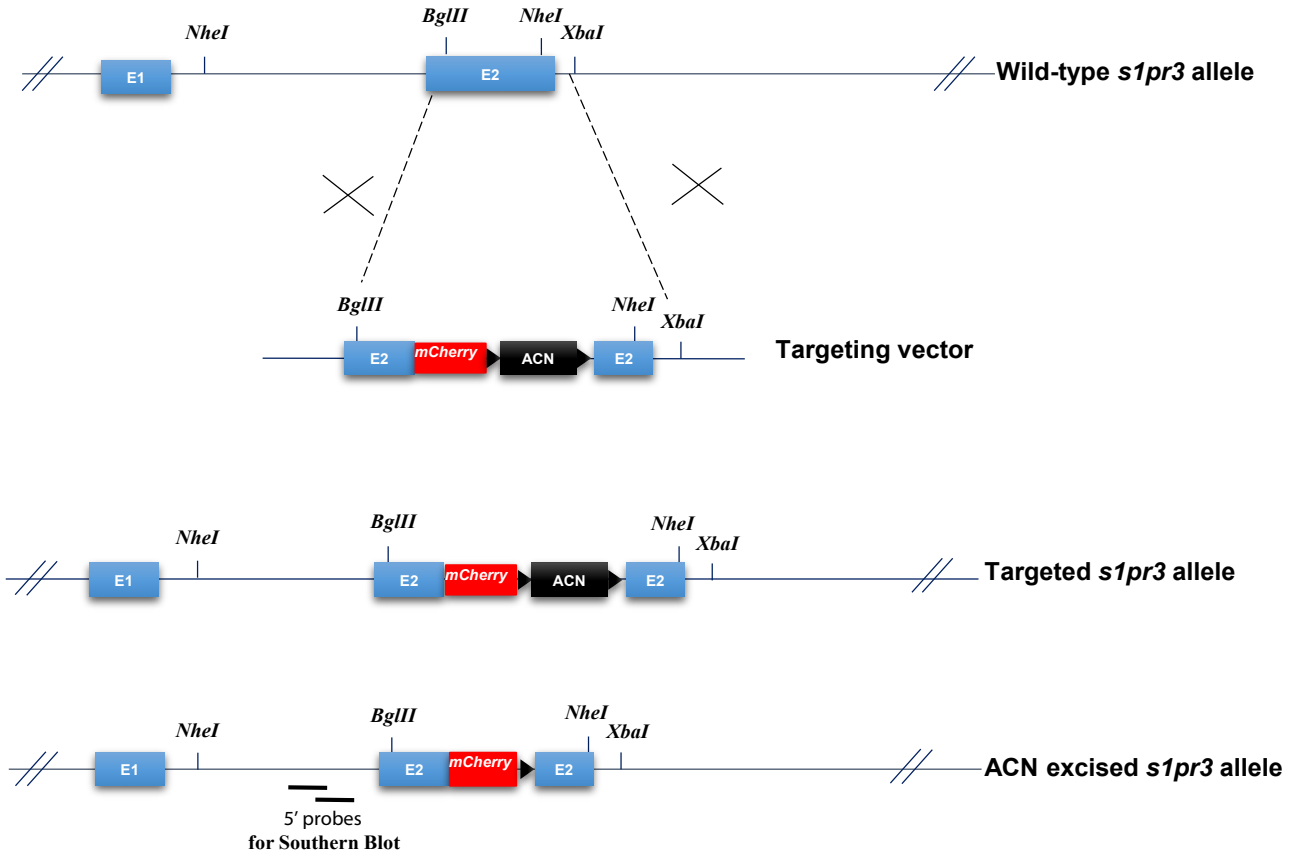
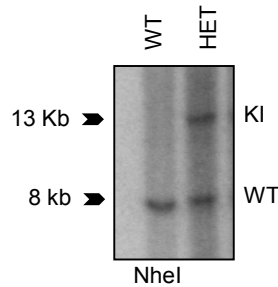
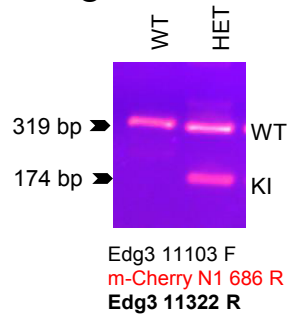




**Supplemental Fig. 3.** Typical chronotropic responses in WT (blue) and S1P3-KO (red) mice to i.p. administration of L-adrenaline (2mg/kg), Isoproterenol/Propranolol (0.1 and 1 mpk, respectively), and Carbamylocholine/Atropine. Heart rates were measured as shown in Methods.

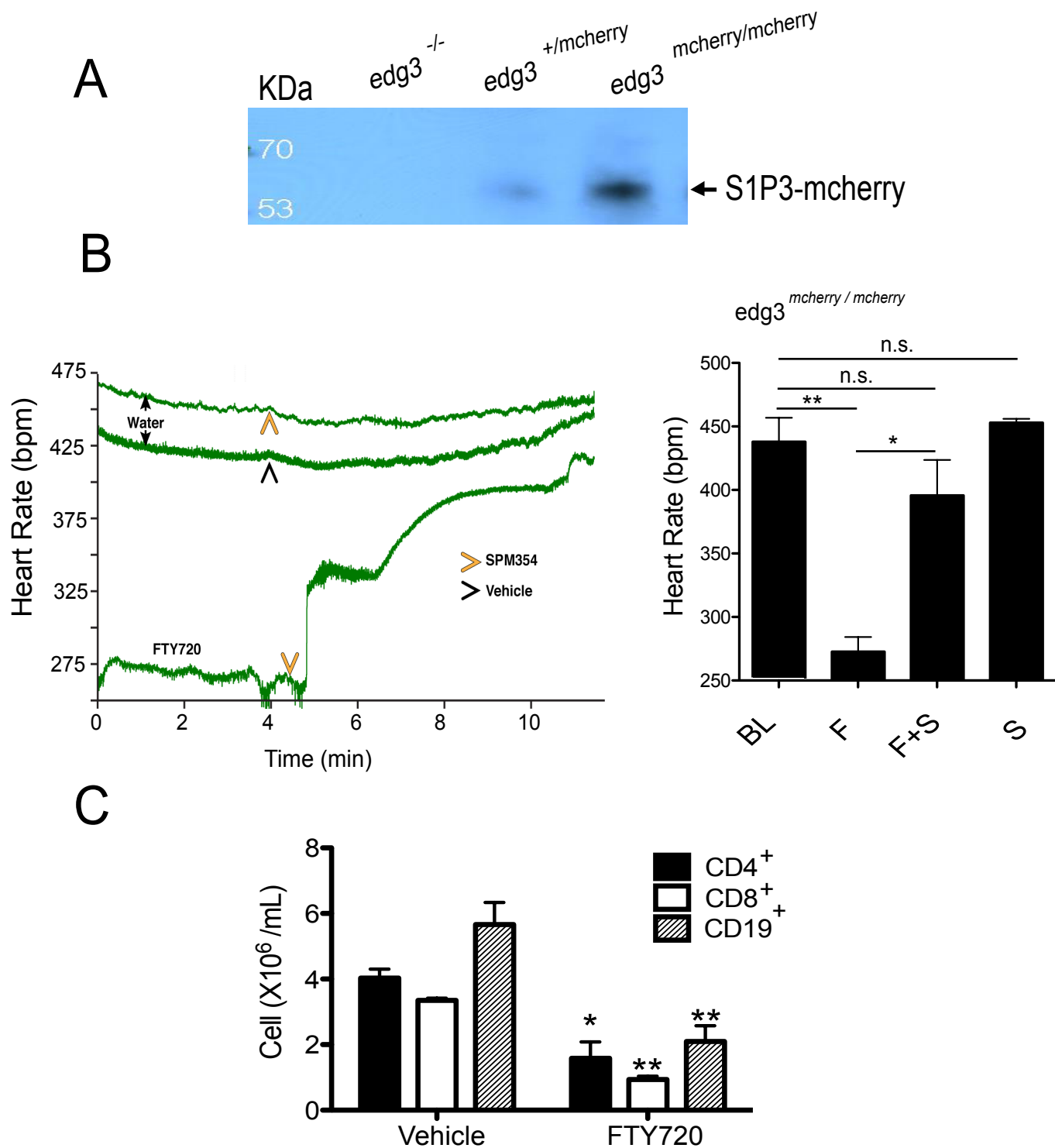


**Supplemental Figure 4.** FTY720-induced bradycardia is not sensitive to W146 reversal. A. Experimental schema. B. Mean heart rate +/- S.E.M. values in mice preadministered with either water vehicle or 20mpk FTY720 for 5h, taken at onset of ECG recording (Baselines), and taken at at experimental end, post W146 and/or SPM354 administration (40 mpk, respectively). The experiment was repeated twice with n=3-4 animals per group. Asterisk indicates Avertin treatment. n.s., not significant.

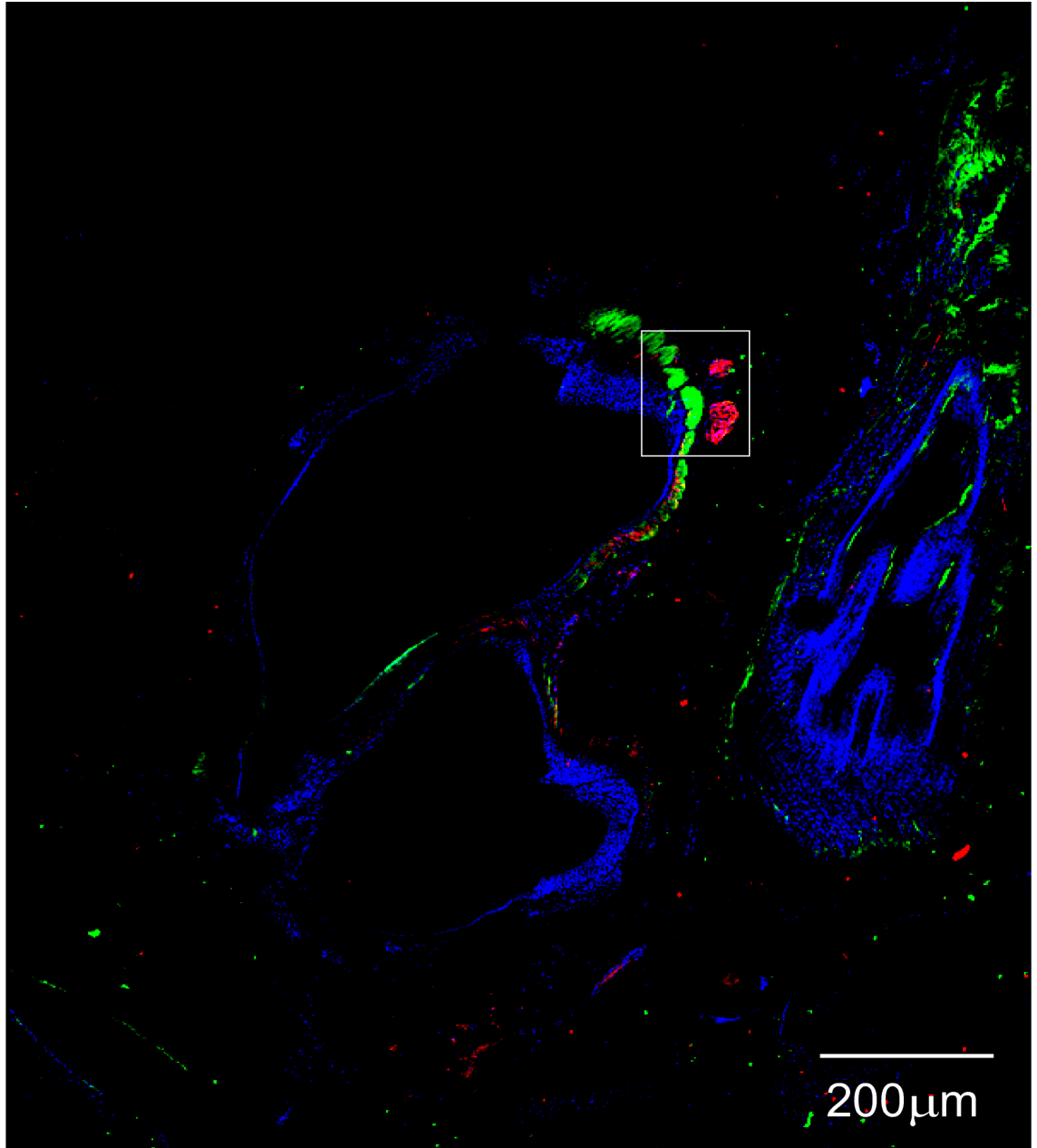

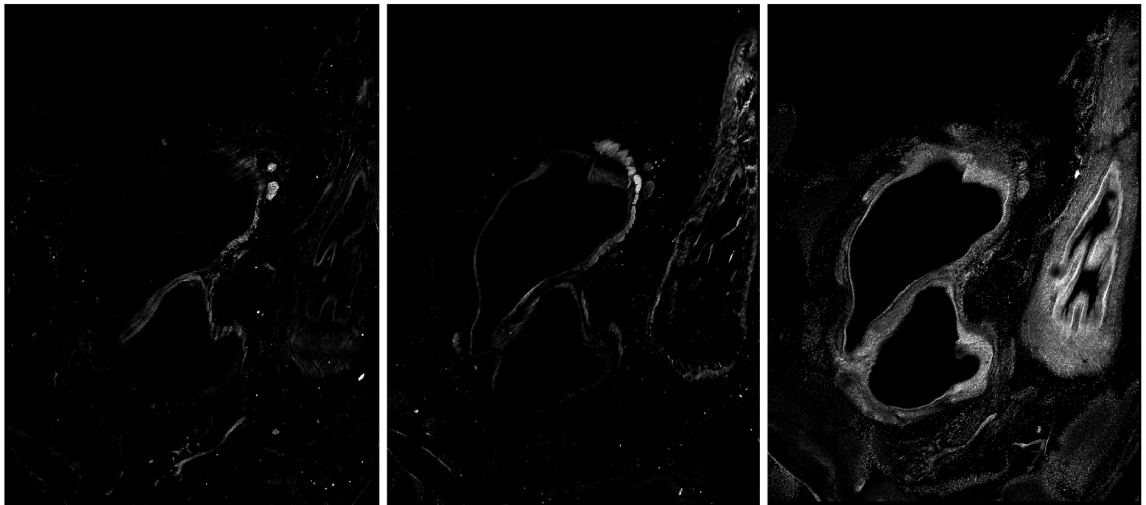
**A****B****C**

**Supplemental Fig. 5. Schematic representation and screening strategy of S1P3 knockin mouse, the making of the of *s1p3 mCherry/mCherry* mouse.**

**A)** Scheme of targeted KI (knockin) plasmid showing generation of *s1p3 mCherry/mCherry* knockin construct. E1 and E2 represent exons 1 and 2 of *s1p3* respectively, ACN signifies the self-excising neomycin resistance cassette. Triangles represent loxP recombination sites. **B)** Southern Blot with EcoRI and NheI digestion of Embryonic Stem Cells (ES cell) DNA of a non-targeted clone following electroporation of the knockin construct. **C)** Genotyping by PCR of chimera mice. These mice were obtained from breeding the chimera C57BL/6J Albino with C57BL/6J. The PCR bands resulting from the WT (319bp) and the KI (174bp) are shown.

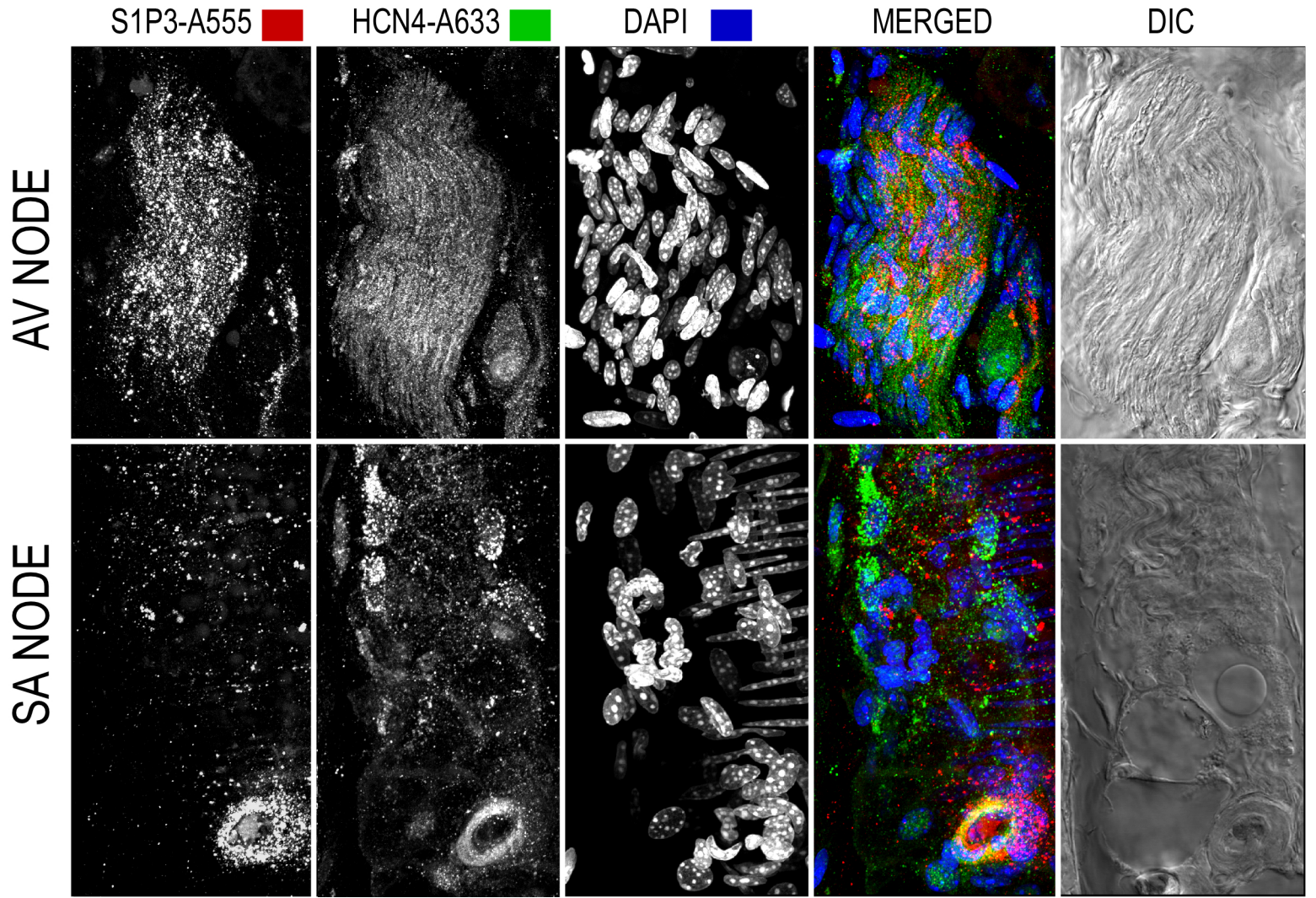


**Supplemental Figure 6.** S1P3 expression and function in the KI mouse. A. Expression of full-length S1P3-mcherry in whole heart lysates from heterozygous (*edg3* <sup>+/mcherry</sup>) and homozygous (*edg3*-mcherry/mcherry) KI mice. B. SPM-354 (F+S) reverses FTY720-mediated bradycardia (F) in KI mice, without altering baseline (BL) heart rate when administered alone (S). C. FTY720 induces blood lymphopenia in homozygous KI mice. Single positive T-cells and CD19 positive B-cell counts are shown in mice treated with water vehicle vs. 5 mpk FTY720 for 5 h.

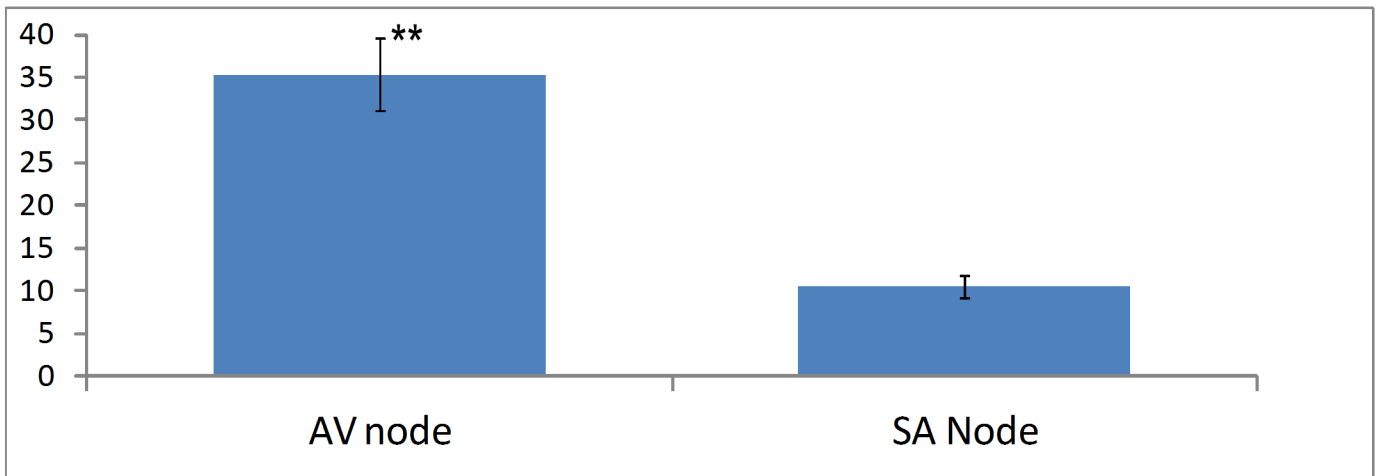
**A**S1P3-A555  HCN4-A633  DAPI S1P3-A555 HCN4-A633 DAPI 

Supplemental Figure 7. High-power confocal view of KI heart with merged S1P3 (red), HCN4, (green) and DAPI (blue) stains, and, respective, single-channel monochromatic images.

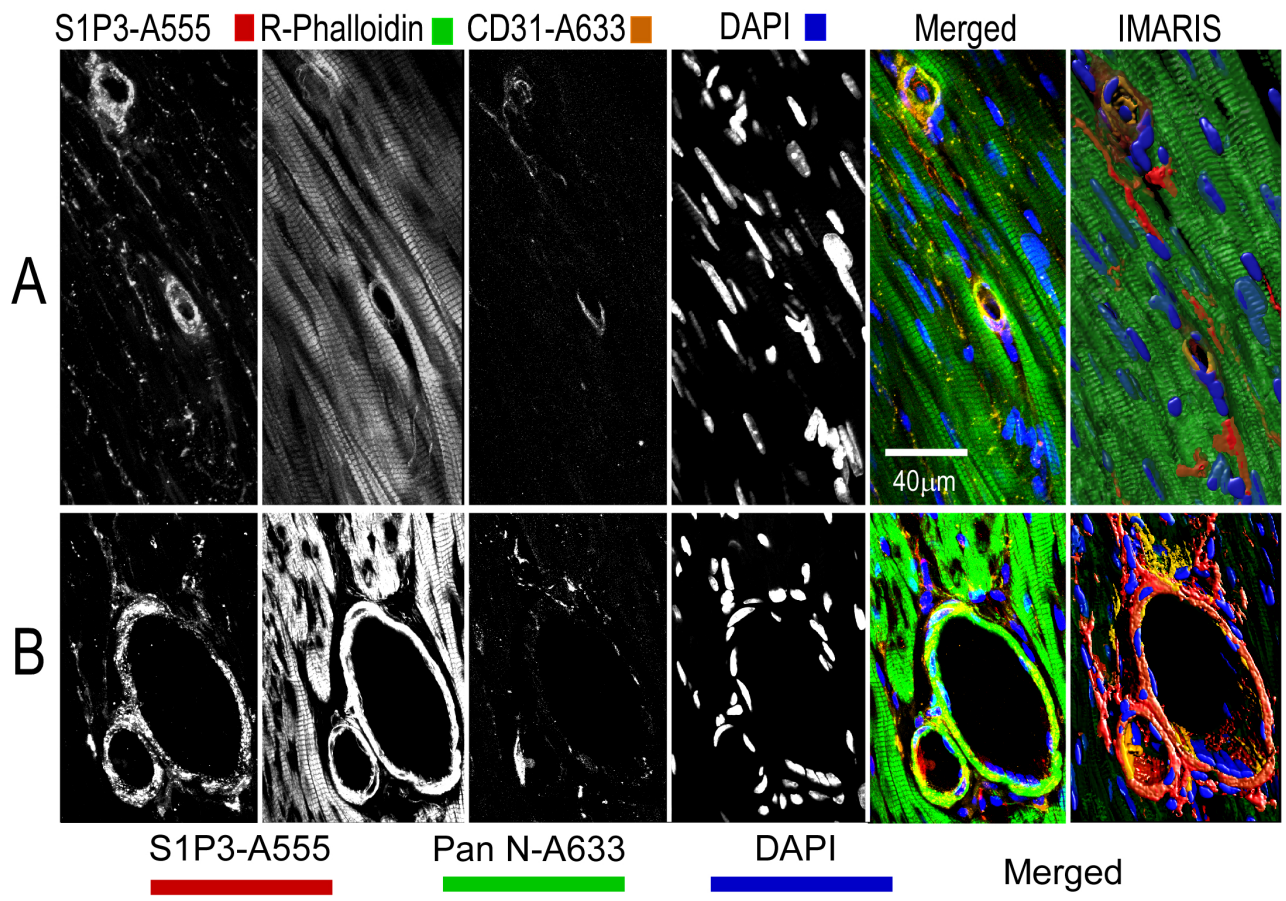
# B



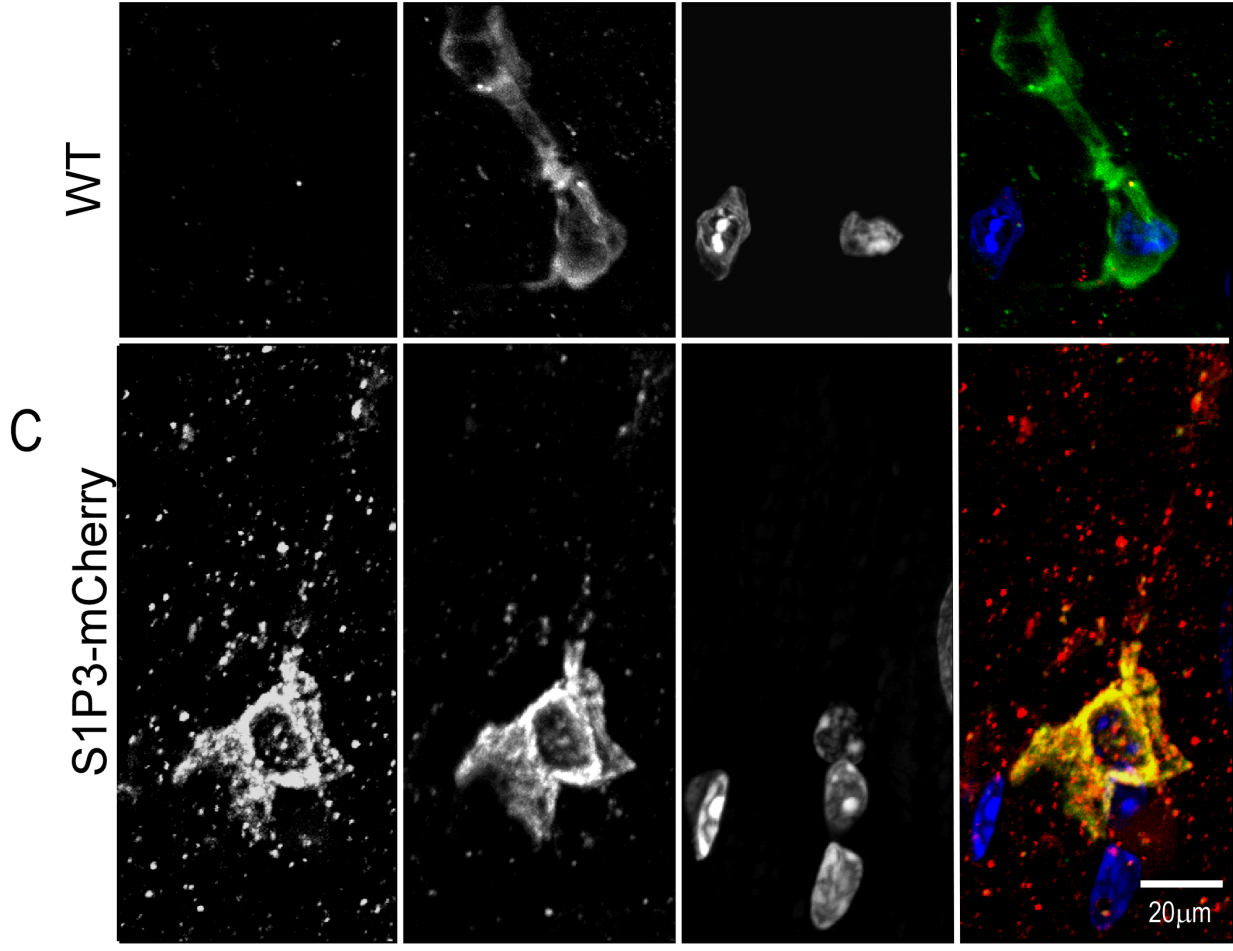
% Area of Fluorescent  
Signal Threshold for S1P3



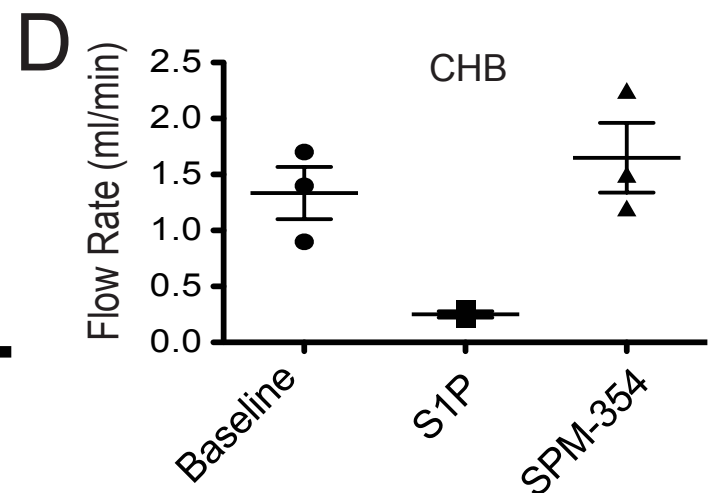
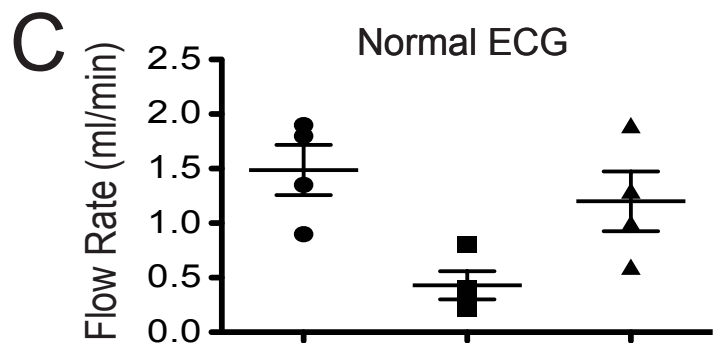
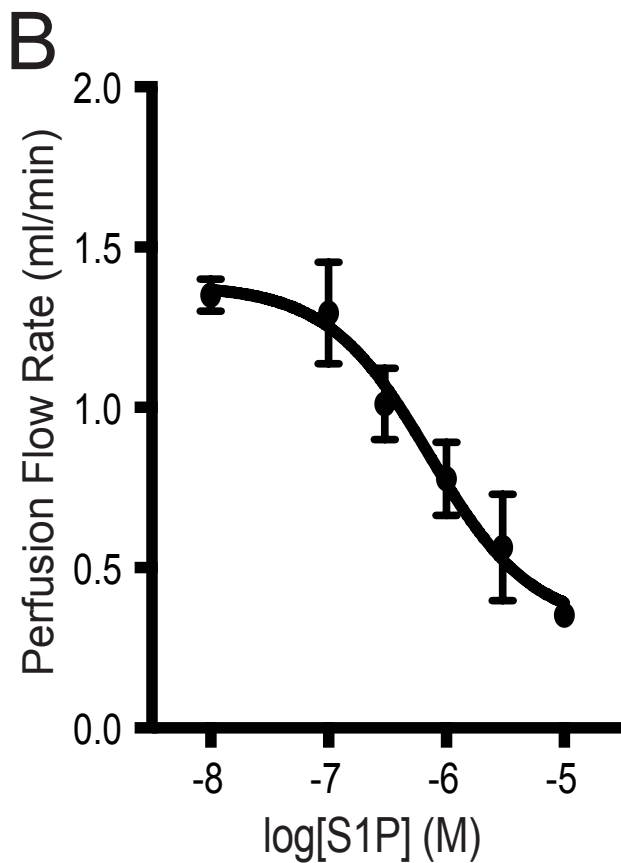
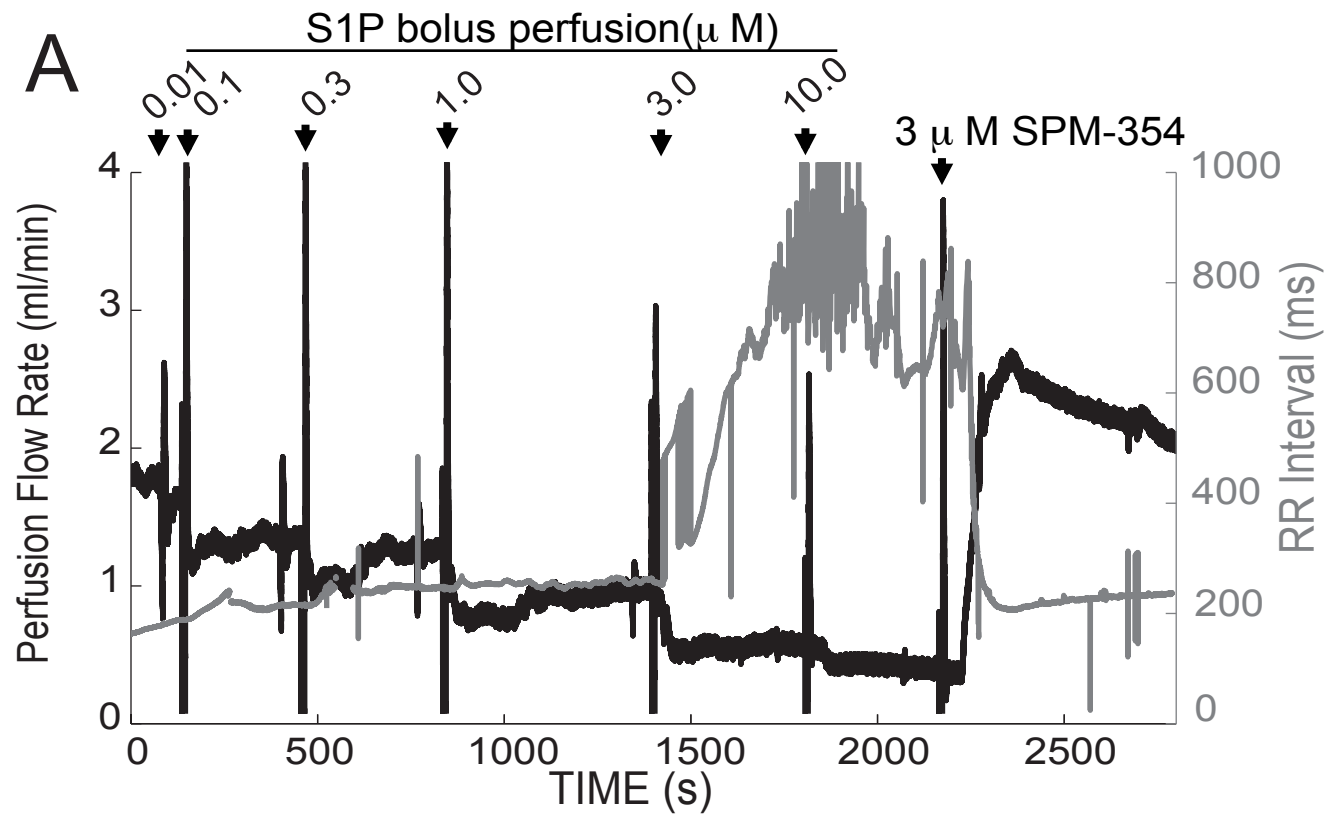
Supplemental Figure 8. Fluorescence quantification of HCN4-and S1P3-mCherry co-expression in AVN and SAN.



S1P3-A555 ■ Pan N-A633 ■ DAPI ■ Merged

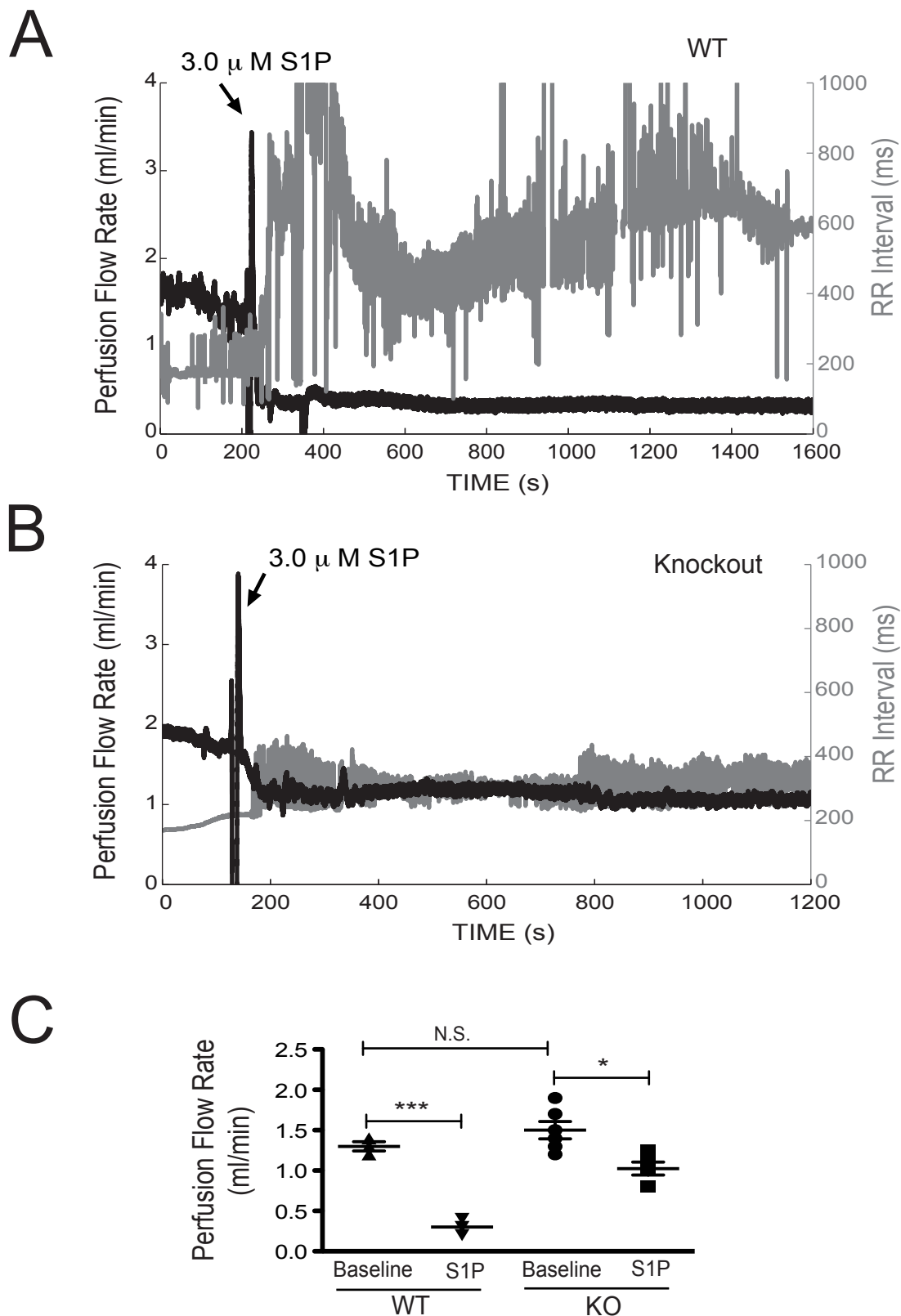


Supplemental Figure 9. Co-expression of mCherry fluorescence with CD31 (A and B) and Pan-neuronal markers (C) in KI mouse ventricle.



**Supplemental Fig. 10.** S1P-induced CHB occurs irrespective of S1P-mediated CF rate reduction. (A) Concentration dependency of S1P-induced CF rate reduction and RR-interval prolongation, which are sensitive to full SPM-354 reversal. (B) Average concentration response curve ( $n=4$ ) of S1P-induced CF rate reduction in mice displaying normal ECG. (C and D) S1P-induced CF rate inhibition and reversal by SPM-354 are intact in mice displaying either normal ECGs ( $n=4$ ) or mice undergoing CHB ( $n=3$ ).





**Supplemental Fig. 11.** Critical dependency of S1P3 on S1P-induced acute RR-interval prolongation. Typical CF rate and RR-interval modulation following 3.0  $\mu$  M S1P bolus perfusion in (A) WT and (B) KO mice, indicate a key contribution of S1P3 on RR-interval prolongation and heart rate variability, largely absent in KO mice. (C) Average  $\pm$  S.E.M. CF rate inhibition maxima to 3  $\mu$  M S1P in WT (n=3) and KO (n=7) mice indicates presence of significant, residual, S1P3-independent decrease in CF rate by S1P.